SKB

TECHNICAL REPORT 98-01

Global thermo-mechanical effects from a KBS-3 type repository

Summary report

Eva Hakami, Stig-Olof Olofsson, Hossein Hakami, Jan Israelsson

Itasca Geomekanik AB, Stockholm, Sweden

April 1998

SVENSK KÄRNBRÄNSLEHANTERING AB
SWEDISH NUCLEAR FUEL AND WASTE MANAGEMENT CO

P.O.BOX 5864 S-102 40 STOCKHOLM SWEDEN
PHONE +46 8 459 84 00
FAX +46 8 661 57 19

GLOBAL THERMO-MECHANICAL EFFECTS FROM A KBS-3 TYPE REPOSITORY

SUMMARY REPORT

Eva Hakami, Stig-Olof Olofsson, Hossein Hakami, Jan Israelsson

Itasca Geomekanik AB, Stockholm, Sweden

April 1998

GLOBAL THERMO-MECHANICAL EFFECTS FROM A KBS-3 TYPE REPOSITORY

Summary Report

Prepared by:

Eva Hakami
Stig-Olof Olofsson
Hossein Hakami
Jan Israelsson

Itasca Geomekanik AB
Stenbocksgatan 1
114 30 Stockholm

Prepared for:

SKB
Box 5864
102 40 Stockholm

April 1998

Keywords: Thermo-Mechanical Effects, 3DEC Modeling, Global, Repository, Stresses, Temperatures, Fracture zones

ABSTRACT

The objective of this study has been to identify the global thermo-mechanical effects in the bedrock hosting a nuclear waste repository — i.e., the effects at large distances from the repository. Numerical thermo-mechanical modeling was performed in several steps, beginning with elastic continuum models and followed by distinct element models (*3DEC*), in which fracture zones are explicitly simulated. The number of fracture zones, the heat intensity of the waste, the material properties of the rock mass and the boundary conditions of the models were varied in different simulations.

To investigate the influence of repository layout, different models for multi-level repositories were also analyzed and compared to the main single-level case. Further, the global influence from the excavation of repository tunnels and deposition holes was examined by introducing weaker rock mass material properties in the repository region of one model. These equivalent properties of the repository region were estimated by numerical modeling of a single repository tunnel.

The results from the numerical modeling show that the principal stresses increase near the repository. The maximum stress obtained for the main model is 44 MPa and occurs at the repository level after about 100 years of deposition. Due to thermal expansion, the rock mass displaces upward, and the maximum heave at the ground surface after 1000 years is calculated to be 16 cm. In the area close to the ground surface, above the center of the repository, the horizontal stresses reduce, causing the rock to yield in tension down to a depth of about 80 meters.

In correspondence with the stress changes, the fracture zones show opening normal displacements at shallow depths and closing normal displacements and shearing at the repository level. The maximum displacements of the different fracture zones are 0.3–2.5 cm for closing, 0.0–0.8 cm for opening and 0.2–2.2 cm for shearing.

The resultant stresses and displacements depend in large part on the assumptions made concerning the heat intensity of the waste. In the main model, an initial heat intensity of 10 W/m^2 is assumed. This thermal load results in clearly larger thermo-mechanical effects than, for example, does 6 W/m^2.

Another important input parameter for the analysis is the Young's modulus of the rock mass. In the main model, a value of 30 GPa is assumed. Higher values of Young's modulus give larger thermo-mechanical effects. Other

changes of the properties considered give minor changes of the rock mass behavior.

All multi-level repository layouts give rise to higher temperatures than the single-level layout, causing the compressive stresses to increase more at the repository level. (Initial heat intensity was the same on each repository level, 10 W/m^2). The multi-level layouts also cause a destressed zone extending in depth well beyond that induced by a single-level layout. Fracture zone displacements caused by different layouts are fairly similar.

The *3DEC* model with altered properties at the repository region (analyzed to evaluate the influence from excavation openings) shows very similar results to the main model. The global effect from the excavated repository tunnels and deposition holes is therefore not significant. However, further numerical computations with repository tunnels and deposition holes modeled explicitly are needed to study the local thermo-mechanical response in the repository region.

SAMMANFATTNING

Målsättningen med denna studie har varit att identifiera de globala termo-mekaniska effekterna i berggrunden omkring ett slutförvar för kärnavfall, dvs effekterna på ett stort avstånd från förvaret. Studien var upplagd i flera steg, med elastiska kontinuummodeller i ett första steg som följdes av distinkt-element-modeller (*3DEC*) där sprickzoner simuleras. Antalet sprickzoner, värmeintensiteten hos avfallet, bergmassans material-egenskaper och randvillkoren i modellerna varierades.

För att undersöka inverkan av förvarets utformning, analyserades även olika modeller med förvar i flera nivåer. Dessa jämfördes med huvudmodellen med en förvarsnivå. Dessutom studerades den globala inverkan som kan förväntas från utbrytningen av förvarstunnlar och deponeringshål genom att svagare materialegenskaper tillskrevs förvarsområdet i en modell. Dessa ekvivalenta egenskaper för förvarsområdet bestämdes genom numerisk modellering av en enskild förvarstunnel.

Resultaten från den numeriska modelleringen visar att huvudspänningarna ökar i närheten av förvaret. Den största bergspänningen som fås i huvudmodellen är 44 MPa och uppträder på förvarsnivå efter omkring 100 år efter deponering. På grund av den termiska expansionen förskjuts bergmassan uppåt och den största hävningen vid markytan efter 1000 år beräknas till 16 cm. I området närmast markytan, ovanför förvarets mitt, reduceras spänningarna så att plasticering sker i bergmassan ner till ca 80 m djup.

I överensstämmelse med spänningsförändringarna uppvisar sprickzonerna öppnande normalförskjutningar närmast markytan, och slutande normalförskjutningar och skjuvning närmare förvarsnivån. Den maximala storleken på förskjutningen av de olika sprickzonerna är 0.3-2.5 cm för slutande normalförskjutning, 0.0-0.8 cm för öppnande normalförskjutning och 0.2-2.2 cm för skjuvning.

Spännings- och deformationsberäkningarna är mycket beroende av de antaganden som görs avseende värmeintensiteten hos avfallet. I huvudmodellen har en initiell intensitet på 10 W/m^2 antagits. Denna termiska last resulterar i klart större termo-mekaniska effekter än vad till exempel 6 W/m^2 gör.

En annan viktigt ingångsparameter för analysen är elasticitetsmodulen i bergmassan. I huvudmodellen antas värdet 30 GPa. Högre värden på elasticitetsmodulen ger större termo-mekaniska effekter. Andra förändringar

i materialegenskaper som studerats ger mindre skillnader i bergmassans uppträdande.

Alla modeller med förvar i flera nivåer ger högre temperaturer än huvudmodellen med en nivå, och orsakar att tryckspänningarna stiger mera vid förvaret i dessa modeller. (Initiella värmeintensiteten är densamma på varje enskild förvarsnivå, 10 W/m^2). En utformning med flera nivåer ger även upphov till att det spänningsrelaxerade området går ner betydligt djupare än vad som är fallet med en förvarsnivå. Rörelserna hos sprickzonerna är likartade för de olika utformningarna.

3DEC-modellen med förändrade materialegenskaper i förvarsområdet, som analyserades för att undersöka inverkan av utbrutna rum, visar på nästan samma resultat som huvudmodellen. Den globala effekten från utbrutna förvarstunnlar och deponeringshål är därför ej signifikant. Ytterligare numeriska beräkningar, där förvarstunnlar och deponeringshål modelleras explicit, behövs emellertid för att studera den lokala termo-mekaniska responsen i förvarsområdet.

TABLE OF CONTENTS

1 INTRODUCTION

1.1 Background

The Swedish nuclear fuel waste-disposal program plans to build a repository in deep bedrock. The proposed concept for the design of such repository is called KBS-3. In the safety assessment for the future repository, one of the tasks is to examine the expected conditions in the rock mass surrounding the repository. This is important because the rock mass functions as the outer barrier between the radioactive waste and the biosphere.

After the time of deposition, large amounts of heat will still be generated from the waste canisters. With time, the heat will spread out from the repository and cause the surrounding rock to expand. This also implies that the rock stress will redistribute both locally around the repository and at a larger distance on a "global" scale. This study is an attempt to address the global thermo-mechanical effects from a KBS3-type repository.

This report is a summary of the reports by Israelsson *[1995a, 1995b, 1996, 1996b, 1997]* and Israelsson et al. *[1997a, 1997b]*.

1.2 KBS-3 Concept

The PASS study *[SKB, 1992]* concluded that the KBS-3 type repository was the most favorable concept considered, featuring a number of parallel drifts at a depth of approximately 500 m below the ground surface (Figure 1-1). In these drifts, holes with a diameter of approximately 1.6 m and a depth of approximately 8 m are bored vertically in the floor. A canister with the spent fuel surrounded with bentonite is placed in each deposition hole (Figure 1-2). Notice that the canister design has lately been changed, the current diameter of the canister is 1050 mm and the diameter of the deposition hole is consequently 1750 mm. However, this change will have no influence on the results of the calculations other than that the increased circumference will enhance the cooling of the canister.

The spacing of the drifts and the deposition holes are factors that may be adjusted to control the temperature in the rock close to the canisters. The amount and type of fuel in each canister control the heat released from each canister. The preliminary layout includes a tunnel spacing of 40 m, a deposition hole spacing of 6 m, and a thermal output of 1000-2500 W per canister.

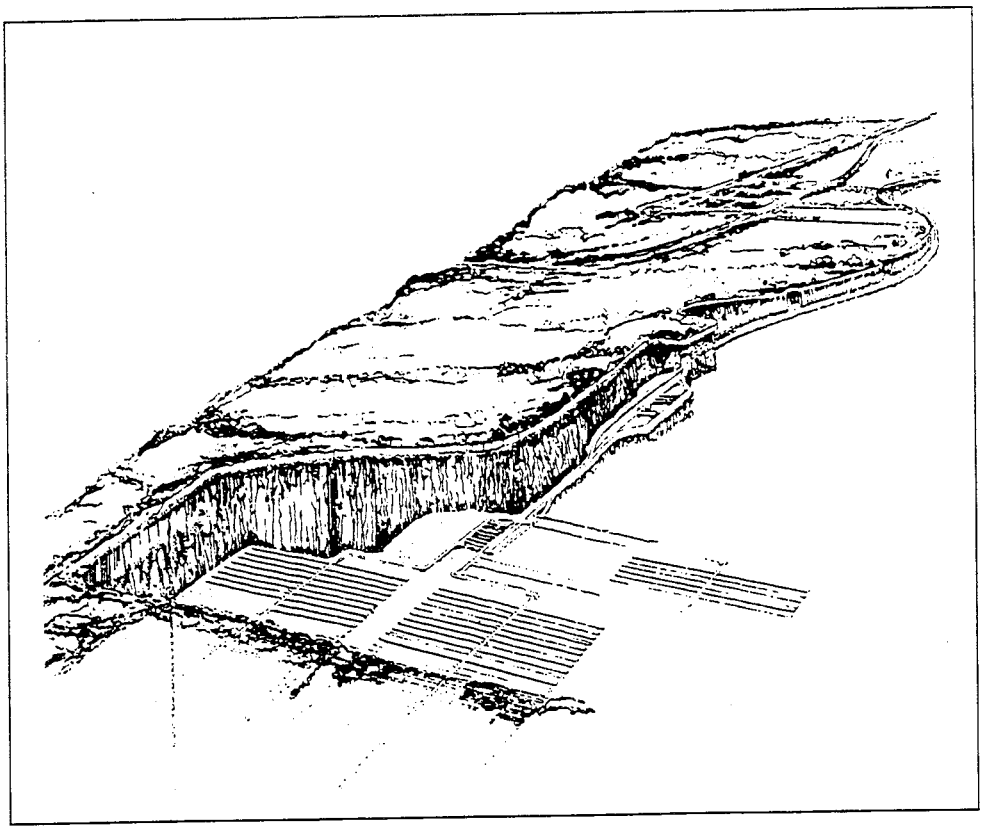

Figure 1-1 *A KBS-3 type repository.*

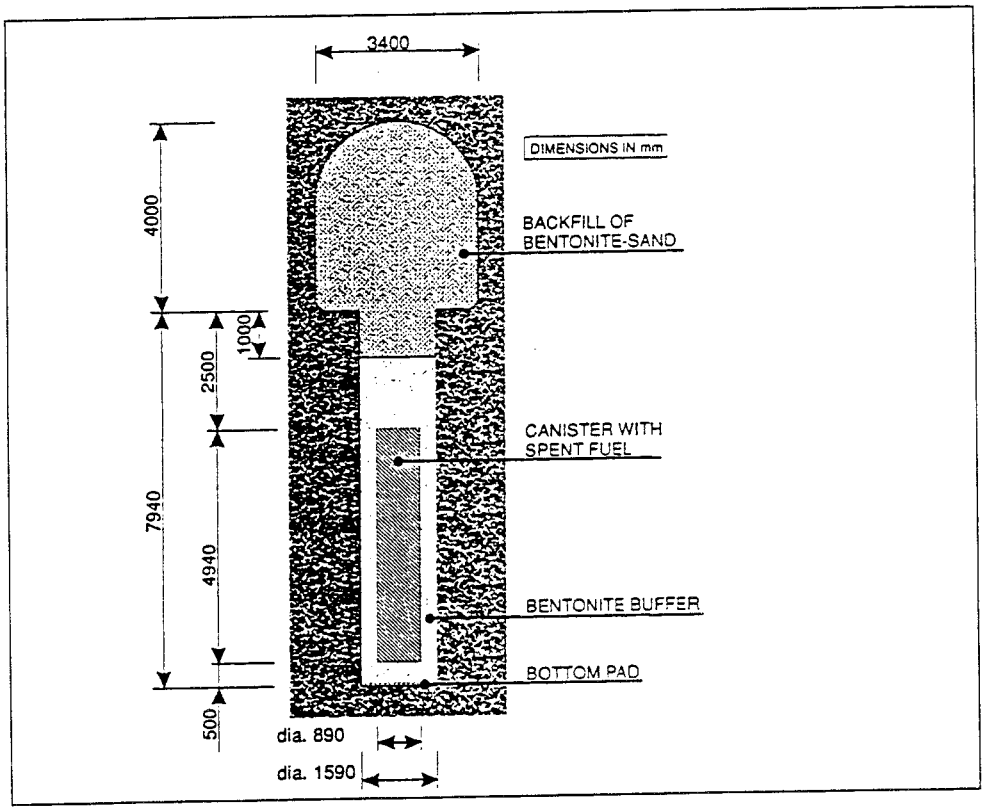

Figure 1-2 *Deposition hole geometry.*

SKB has adopted a characterization scheme for discontinuities *[Almén et al., 1996]*. Discontinuities are divided in four orders based on their anticipated influence on the repository design. Discontinuities of the first and second order must, according to the scheme, not cut through the repository area. Thus, depending on the total amount of waste and the regional geology of the actual site, the repository may have to be divided into several parts or separate levels. In this study, it is assumed that the single-level repository has an areal extension of one square kilometer.

1.3 Objectives

The global thermo-mechanical effects from storing heat-generating spent nuclear fuel in the bedrock are difficult to predict precisely. The rock volume involved is very large and, even with extensive investigations, the detailed properties of the rock and the discontinuities would remain largely unknown. In addition, there is no previous experience from such heat-generating waste disposal. Therefore, the objectives of this study have been to use the existing knowledge of rock material and existing mathematical tools to try to identify, and possibly quantify, the thermo-mechanical effects that can be expected.

While the study is not site-specific, an example of a realistic rock mass, the geology of Äspö, was used as a base for the model set-up.

1.4 Modeling Approach

The bedrock consists of rock material of varying composition, intersected with discontinuities of different types at all scales (cracks, joints, faults, fracture zones). The mechanics of such a fractured medium cannot be modeled without considerable simplifications.

In the first models, the rock was assumed to be a linear elastic continuum with isotropic and homogenous properties *[Israelsson, 1995a,b]*. The numerical code *STRES3D [St. John and Christianson, 1980]* was applied for the analyses. *STRES3D* is a semi-analytical computer code for thermo-elastic analyses for various cases of heat sources (in half-space). The *STRES3D* models were used to analyze the change in temperature and stress distribution with time for different heat intensities and thermal conductivities of the rock mass.

In subsequent modeling *[Israelsson, 1996a,b; 1997; Israelsson et al. 1997a,b]*, the numerical code *3DEC* (3-Dimensional Distinct Element Code) *[Itasca, 1994]* was used. Using this code, further realism was introduced to the analysis by simulating the mechanical influence of major fracture zones in the repository area. *3DEC* models the response of a discontinuous medium (such as a fractured rock mass) as an assemblage of discrete blocks. The discontinuities are treated as interfaces between blocks,

and each block is divided into a mesh of finite-difference elements. The behavior of the elements follows predefined constitutive laws.

Because the modeling requires simplifications concerning rock mass behavior, there is an uncertainty in the selection of appropriate material models and associated parameters. Where accurate parameters have been difficult to determine, a conservative approach has been taken — i.e., the parameters were selected such that the thermo-mechanical effects would not be underestimated. No effects from the groundwater are taken into account.

Due to the necessary simplifications and the uncertainty in selecting some of the input parameters, the modeling work took on the nature of a "sensitivity" exercise. Series of models with one or more features changed were analyzed and compared with each other (see Table 1-1). In this report, one of the *3DEC* models is referred to as the "main" model, as this is the model which is judged to be the most realistic in terms of rock mass properties. The properties of the main model will be described first in Section 2 - 4. Section 5 gives a presentation of the results from the main model and the multi-level models. This section also illustrates the influence on results from initial heat effect and thermal conductivity. Thereafter, in Section 6, the major findings from the comparison between the models with modified number of fracture zones, mechanical material properties and boundary conditions, will be presented.

Table 1-1. Numerical analyses performed

Numerical code	Modified property	Parameter values used
STRES3D	Initial heat intensity	6, 6.9 and 10 W/m²
	Thermal conductivity of rock mass	c = 3.0 and 3.7 W/m °C
3DEC	Number of fracture zones	2, 4 and 9
	Boundary condition on vertical boundaries	Fixed normal displacement and fixed normal stress
	Tensile strength of rock mass	0 and 8.7 MPa
	Young's modulus	30 and 60 GPa
	Repository layout	1,2 and 3 levels
	Material property in repository region	Equal to surrounding rock and "equivalent" properties (see Section 6.4)

2 MODEL GEOMETRY

2.1 *STRES3D* model

In *STRES3D*, the stress, displacement and temperature results may be calculated at single points, along lines or in a grid, as specified by the user. For this project, the results were calculated along four lines, as given in Figure 2-1.

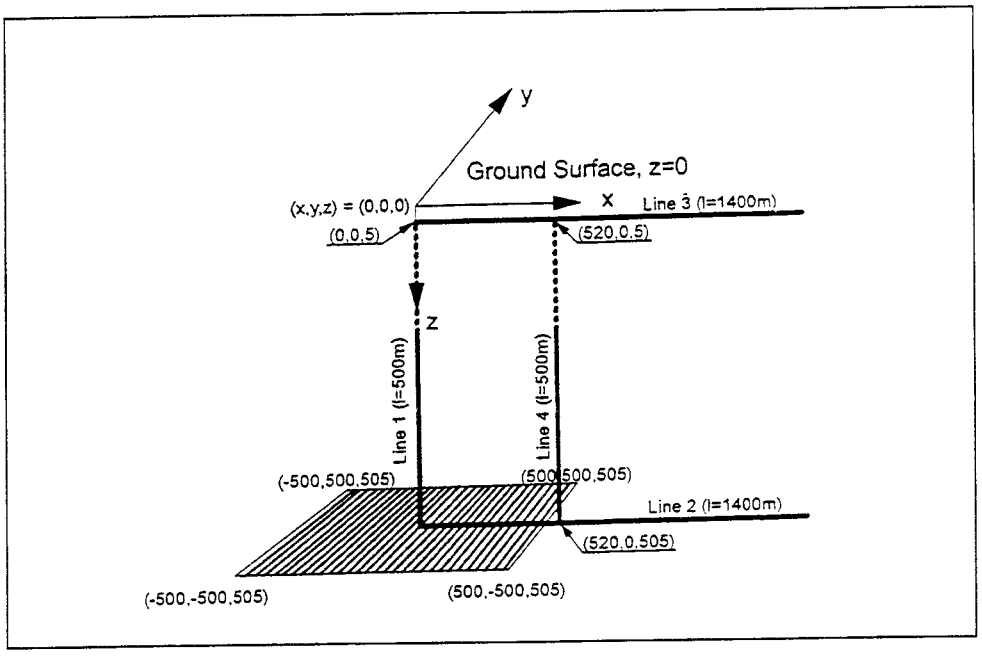

Figure 2-1 *Lengths, location and orientation of monitoring lines in the STRES3D models.*

Each canister is modeled as a single-point heat source located at the center of the canister. The point sources were distributed over a square area of 1 km by 1 km at a depth of 500 m below ground surface. The spacing between tunnels is assumed to be 40 m; the spacing between canisters along the tunnel is assumed to be 6 m.

2.2 *3DEC* model

The *3DEC* models were built within a block of 4000 x 4000 x 2000 m in size (see Figure 2-2). This block has a fine element discretization close to the repository and a coarse mesh in the outer regions. For the model with a

single repository level (main model), the area at the repository has an even finer discretization. The sides of the block are oriented parallel to the principal in-situ stress directions (see Section 4.1).

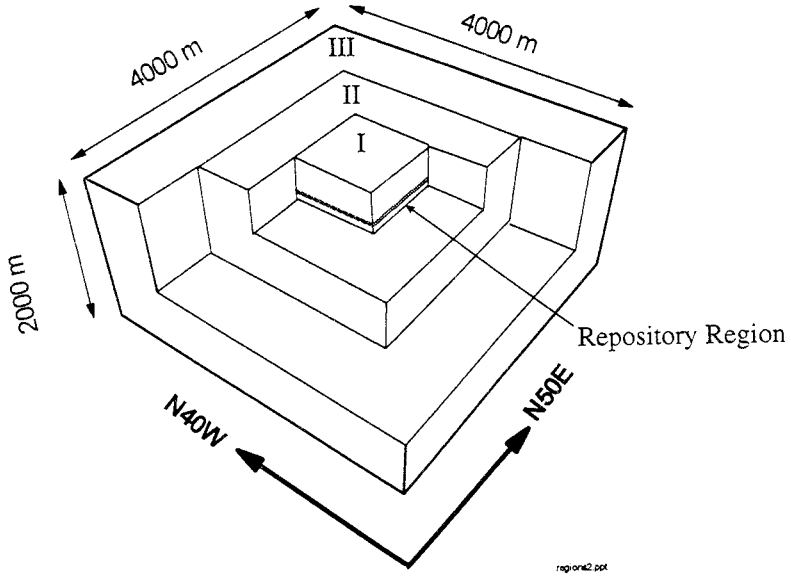

Figure 2-2. *3DEC model geometry and discretization regions. (Blocks in the foreground are hidden to reveal the inner parts of the model.)*

Figure 2-3 shows the location and orientation of the fracture zones considered in the 3DEC model. It can be noted that most zones are steeply dipping and oriented northeast-southwest. The names of the fracture zones originate from the SKB Äspö fracture network, from which the most dominating fracture zones were selected to be included in the model *[Gustafson et al., 1991; Munier and Sandstedt, 1994; Windelhed et al., 1995].*

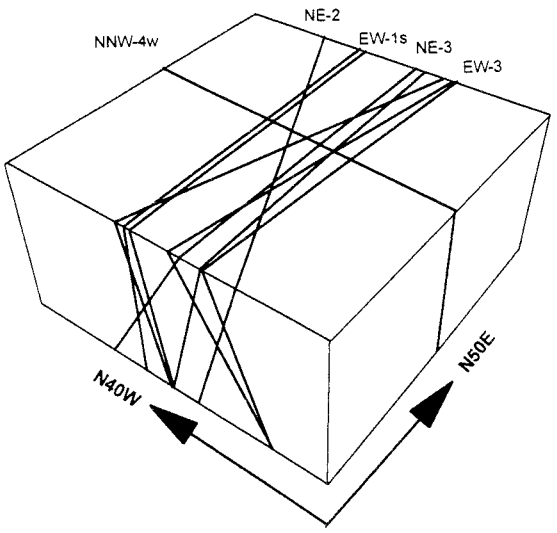

Figure 2-3. *Model orientation and fracture zone geometry.*

The repository was simulated as a grid of point heat sources, identical to the *STRES3D* model. The location of the repository in the main model with respect to the fracture zones is given in the Figure 2-4.

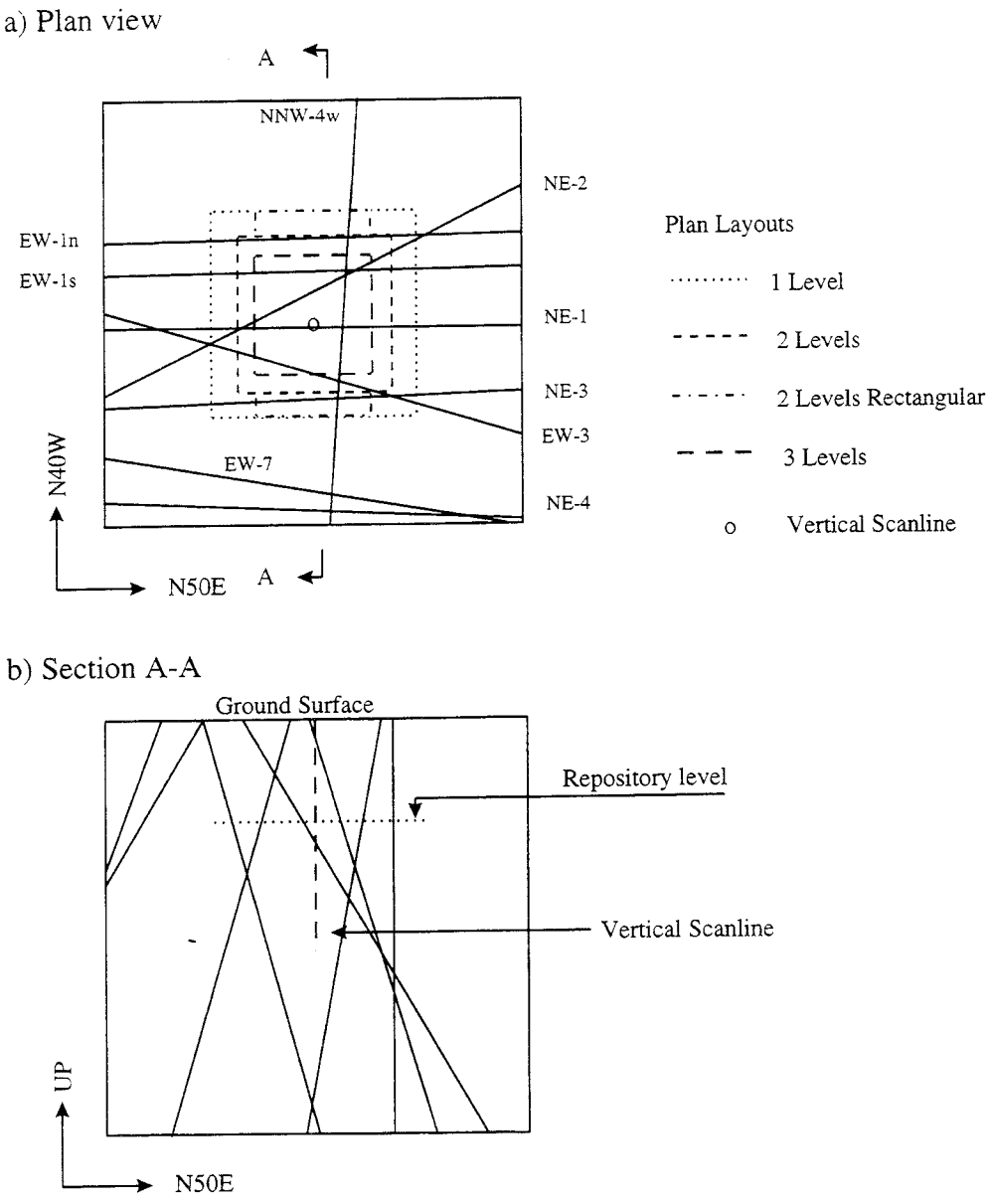

Figure 2-4. a) *Plan view the fracture zone network at 500-m depth together with the outlines of repositories and the location of the scanline (Central part, cf. Figure 2-2). b) Vertical section through the model showing the fracture zone intersecting and the location of a single-level repository (Central part, cf. Figure 2-3).*

The location of heat sources was different in the model for the single-level repository (main model) and the multi-level cases. In total, seven different repository layouts have been compared. The thermal load area and the

initial areal heat intensity was kept the same in each repository level for all lay-outs (i.e. the heat sources are more densely distributed in the multi-level cases). Table 2-1 gives the configuration of the different repository layouts analyzed.

Table 2-1. Repository layouts analyzed in this study.

Number of levels	Length of repository boundaries (m)	Distance between levels (m)	Depth to upper level	Total no. of canisters	Case Identifier
1	1000 x 1000	—	500	4 368	1_SQ
2	680 x 714	50	500	4 320	2_50
2	680 x 714	100	500	4 320	2_100
2	680 x 714	150	500	4 320	2_150
2	520 x 918	100	500	4 312	2_REC
3	600 x 534	50	500	4 320	3_50
3	600 x 534	100	500	4 320	3_100
3	600 x 534	150	400 *	4 320	3_150

* Note that the top of the uppermost level of this layout lies at 400-m depth.

The effects from the excavations in the repository (tunnels and deposition holes) were not considered in the main model. The volume of excavated rock is small compared to that of the surrounding rock; therefore, the openings were not expected to influence greatly the thermo-mechanical effects on a global scale. This issue was addressed, however, in a separate analysis (see Section 6.4).

3 THERMAL MODEL

3.1 Heat-intensity function

The heat-release function applied is defined by the following equation *[Thunvik and Braester, 1991]* (also shown in Figure 3-1):

$$Q(t)/Q_0 = \left(\alpha_1 e^{-\alpha_2 t} + (1-\alpha_1)e^{-\alpha_3 t}\right) \qquad (3\text{-}1)$$

where $Q(t)$ denotes the time-dependent heat intensity,
Q_0 denotes the heat intensity at the time of the deposition,
t is the time,
$\alpha_1 = 7.531212\text{x}10^{-1}$,
$\alpha_2 = 2.176060\text{x}10^{-2}$, and
$\alpha_3 = 1.277985\text{x}10^{-3}$.

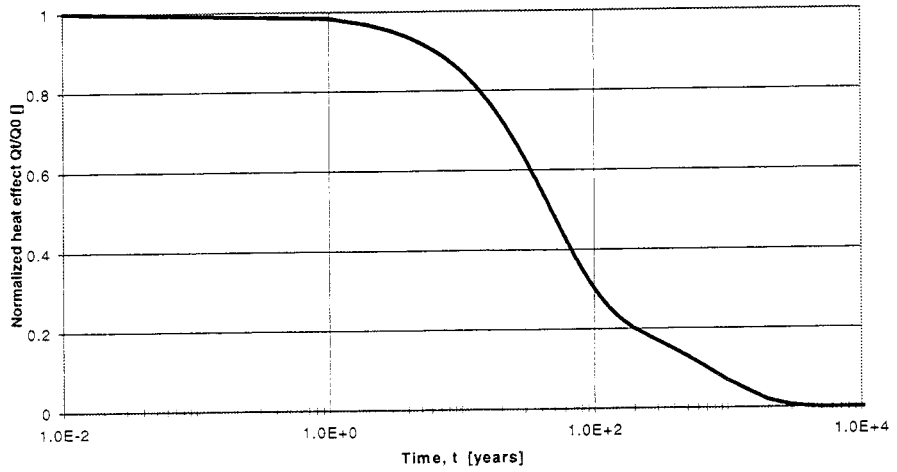

Figure 3-1 *Time-dependent heat decay function of the waste. [Thunvik and Braester, 1991]*

The initial heat intensity at the time of waste deposition (Q_0) is assumed to be 2400 W for the main model, which is considered as an upper bound for canister heat intensity *[Pusch and Touret, 1988; Pusch and Börgesson, 1992]*. With the canister spacing used (40 m x 6 m), the corresponding initial areal intensity becomes 10.0 W/m².

In the model, a conservative assumption was made in assuming that all canisters are deposited at the same time and that they all have the same heat

initial heat intensity. In reality, the repository will be filled with waste slowly such that some of the heat will have been already dissipated when the repository is sealed.

3.2 Thermal boundary conditions

The ground surface was modeled as a fixed temperature boundary. No further boundary condition is considered. (In both the *3DEC* and *STRES3D* models, the temperatures are calculated as if no other boundaries exist). The initial temperatures in the bedrock were assumed to increase with depth with a gradient of 0.016 °C per meter, from 7 °C at the ground surface to about 15 °C at 500 m depth.

3.3 Thermal properties

The thermal properties are assumed to be isotropic and constant throughout the rock block. Thus, the fracture zones do not influence the thermal field. Influences from excavations, filling materials, heat convection by fluid flow or fluid buoyancy were not considered.

In the models, all the material surrounding the point heat sources have the same thermal properties as given in Table 3-1, which are also constant with time. The specific heat and expansion coefficient have been kept the same in all models. The influence of changing the thermal conductivity has been studied by comparing models with a conductivity of 3.0 W/m °C (main model) and 3 .7 W/m °C.

Table 3-1. Thermal properties of the rock mass [after Hansson et al., 1995a,b].

Parameter	Value
Specific heat, *Cp* [J/kg°C]	740.74
Thermal conductivity, *k* [W/m°C]	3.0 (3.7)
Linear expansion coeff., α [1/°C]	8.5E-6

4 MECHANICAL MODELS

4.1 In-situ stress state

The in-situ stress state, as measured at Äspö, is taken to be the initial stress conditions. The major principal stress is nearly horizontal, with a bearing of N40W; the intermediate stress is subhorizontal, and the minor stress is close to vertical. Based on the measured results, the initial stresses were assumed to vary with depth, as given by Larsson *[1995]*:

$$\sigma_H = \sigma_z = 5.0 + 2\sigma_V \tag{4-1}$$

$$\sigma_h = \sigma_x = 2.5 + \sigma_V \tag{4-2}$$

$$\sigma_V = \rho g z = 2700 \cdot 9.81 \cdot z \cdot 10^{-6} \tag{4-3}$$

where z is depth in meters below the ground surface, and stresses are in MPa.

4.2 Mechanical boundary conditions

The upper surface (ground surface) is modeled as a free surface; all other boundary surfaces have zero normal displacement. This boundary condition may influence the fracture zone displacements and give slightly overestimated stresses. Therefore, an analysis was also performed with stress boundary conditions for comparison, as presented in Section 6.

4.3 Constitutive relations

In the *STRES3D* models, the rock has a homogenous, isotropic, linearly elastic behavior. In the *3DEC* models, a Mohr-Coulomb plasticity model was used for the intact rock blocks, and an elastic-plastic constitutive model with Coulomb slip failure was used for the fracture zones.

4.4 Mechanical properties

The input mechanical property parameters used for the rock blocks in the main model are given in Table 4-1. The alternative values are given in parenthesis.

Table 4-1. Rock mass properties used in the models.

Parameter	Value
Young's modulus [GPa]	30 (60)
Poisson's ratio	0.22
Cohesion [MPa]	5
Friction angle [°]	30
Tensile strength [MPa]	0 (8.7)

The width and stiffness assumed for the fracture zones in the *3DEC* models are given in Table 4-2. The stiffness is based on the estimated width of the fracture zones *[Gustafson et al., 1991; Munier and Sandstedt, 1994; Windelhed et al., 1995; Stephansson, 1995]*. The cohesion is assumed to be zero and the friction angle for the fracture zones equal to 20°. The fracture zone stiffness parameters have been kept the same in all analyses.

The knowledge about the mechanical properties of fracture zones is poor, however, because it is difficult to get field information on structures of this size. It can be noted that the fracture zones are here simulated as single continuous features, transecting the entire model.

Table 4-2. Mechanical width and stiffness of the fracture zones.

Fracture zone	Estimated mechanical width [m]	Normal Stiffness, K_n [GPa/m]	Shear Stiffness, K_s [GPa/m]
EW-1n	20	0.50	0.25
EW-1s	20	0.50	0.25
EW-3	15	0.67	0.33
NE-1	30	0.33	0.165
NE-2	10	1.00	0.50
NE-3	20	0.50	0.25
EW-7	10	1.00	0.50
NE-4	15	0.67	0.33
NNW-4w	0.5	20.00	10.00

5 RESULTS

5.1 Temperature distribution

The temperatures were calculated along "scanlines" in the model at specified times after the deposition of the waste — namely, after 50, 100, 200, 400 and 1000 years.

It was found that, at the repository level, the peak temperature was reached at about 200-400 years after deposition. Figure 5-1 shows the development with time of temperatures along a vertical line through the center of the single-level repository. Figure 5-2 shows how the temperature field depends on the assumed thermal load. The three curves represent the cases of an initial areal heat intensity of 6, 6.9 and 10 W/m², respectively. It can be seen that the temperature change scales linearly with the heat intensity when no other parameter is changed. Similarly, the temperature change is inversely linear with the thermal conductivity, when no other parameter is changed (see Figure 5-3).

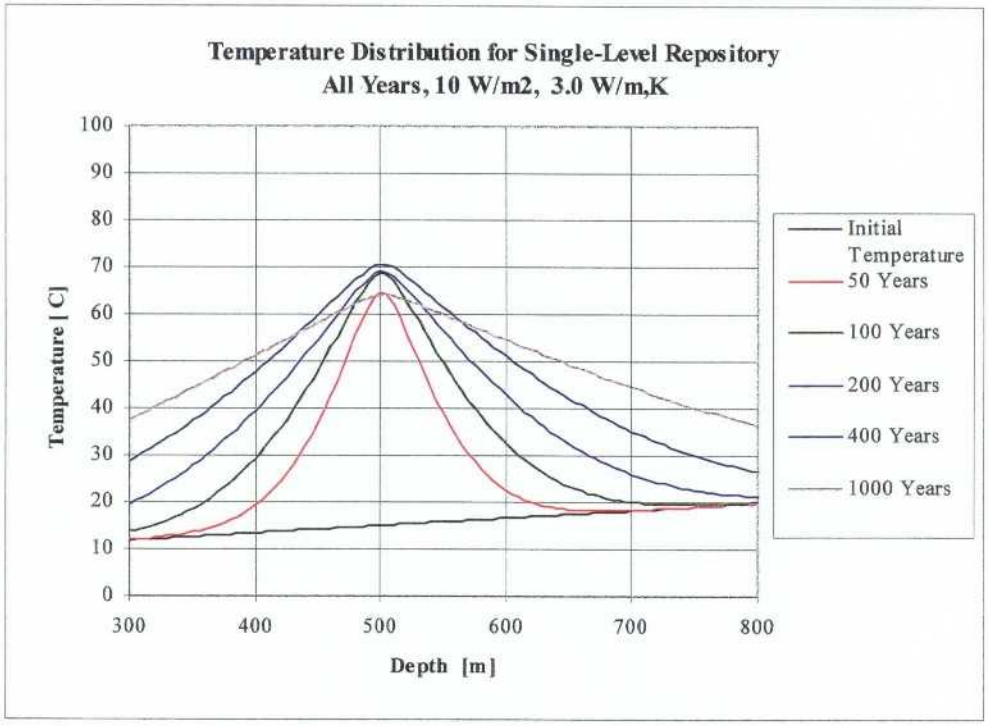

Figure 5-1. *Temperature distribution along vertical scanline through the center of the single-level repository for 0, 50, 100, 200, 400 and 1000 years after deposition. (Results were obtained by using STRES3D.)*

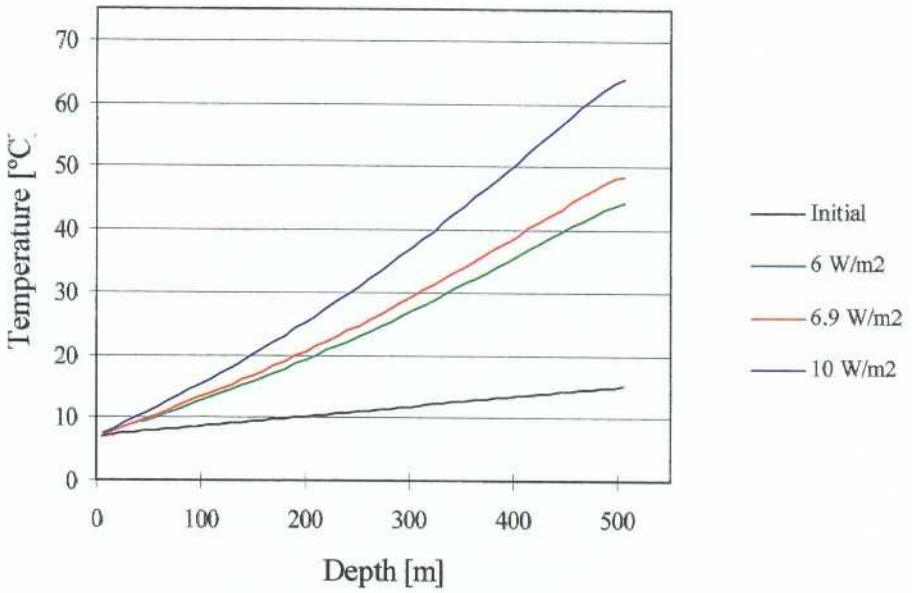

Figure 5-2. *Temperature distribution with depth along a vertical line at the center of a single level repository, initially and after 1000 years of deposition. (Different curves correspond to different values on the initial areal heat intensity; see legend.)*

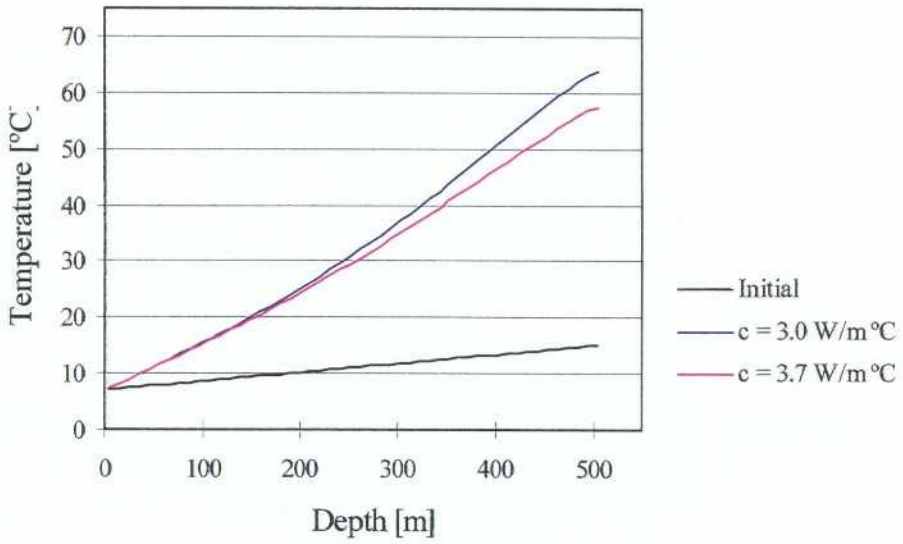

Figure 5-3. *Temperature distribution with depth along a vertical line at the center of a single level repository, initially and after 1000 years of deposition. (Different curves correspond to different values on the thermal conductivity; see legend.)*

Figure 5-4 shows the temperature distribution along the same vertical line for different layouts of the repository. It can be noted that, as expected, the multilevel repositories cause the highest temperatures at the center of the repository. Smaller separation between the levels also gives higher maximum temperatures, due to the influence between the levels. The layout 3-50 (three levels with 50-meter separation) thus causes the highest temperatures among the layouts studied.

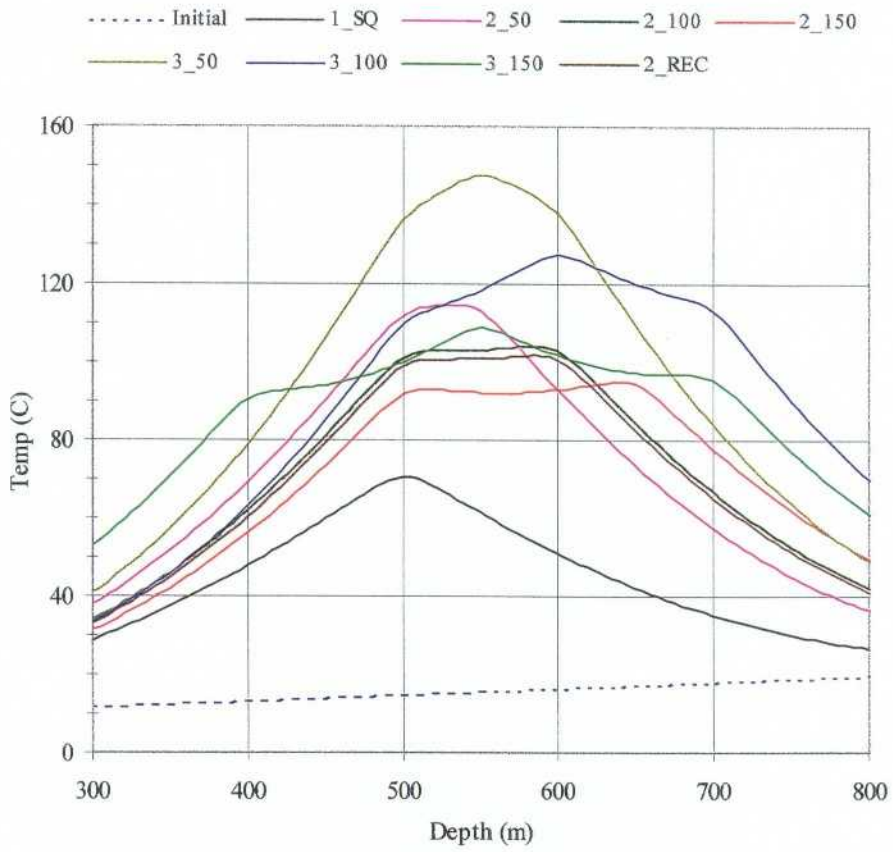

Figure 5-4. *Temperature distribution along vertical scanline through the center of the repository at 400 years after the deposition for the different layouts. (Curve 1-SQ denotes the "main model", with a square single-level repository at 500 meters depth; 2-100 denotes a two-level repository with a 100-meter separation between the levels, etc. Results were obtained by using STRES3D.)*

5.2 Thermally induced stresses in the *3DEC* models

The calculated stresses for each time analyzed were collected at element zone centroids closest to the specified points along the vertical scanline. Figures 5-6 and 5-7 shows how the principal stresses change with time along this vertical line. Because the element zones are fairly large, the centroid locations do not match perfectly to the scanline, which results in the slightly jagged curves of stress versus depth. Some of the stress changes are also caused by the fracture zones intersecting the scanline.

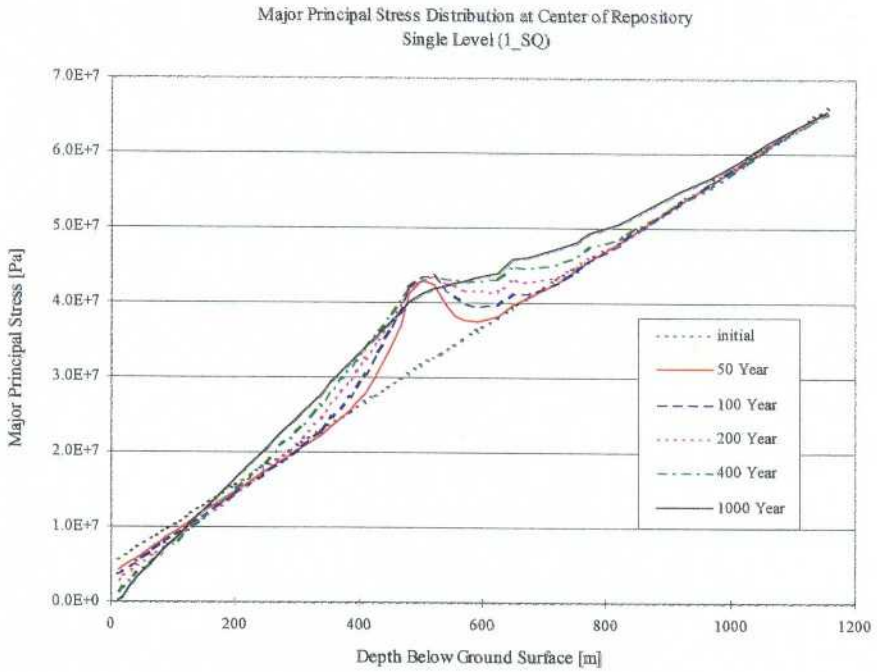

Figure 5-5. *Major principal stress versus depth along the vertical scanline. (The different curves refer to different times after deposition (see legend). The single-level repository lies at 500-meter depth below ground surface, 1-SQ.)*

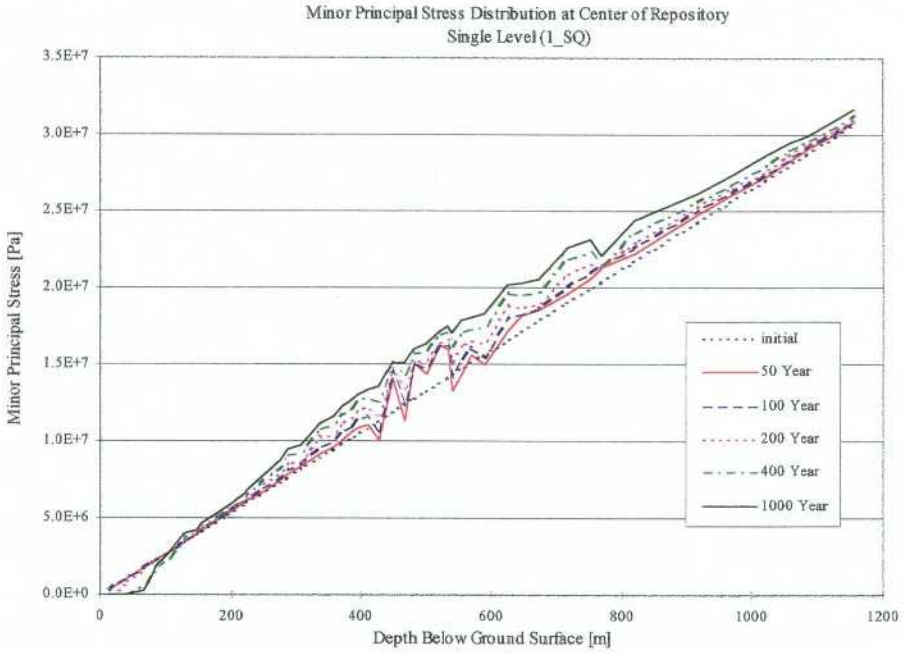

Figure 5-6. *Minor principal stress versus depth along the vertical scanline. (The different curves refer to different times after deposition (see legend). The single-level repository lies at 500-meter depth below ground surface, 1-SQ).*

After 50 years of deposition, an increase in major principal stress of about 12 MPa is calculated, at the level of the repository. Between the times 400 and 1000 years after deposition the major stress, in this area, starts to decrease slowly and at 1000 years the major stress lies about 10 MPa higher than the initial stress.

In areas far from the repository, the stress changes are largest at the latest time analyzed (1000 years). Also, the change in minor principal stress continues to increase within the time span analyzed. At 1000 years, the minor stress has increased about 4 MPa at the level of the repository (see Figure 5-6).

In the rock mass close to the ground surface, the principal stresses decrease compared to the initial state of stress. At 1000 years, the major principal stress has decreased to about zero from the initial value of 5 MPa. During the thermo-mechanical process, there is also a reorientation of principal stresses such that the minor principal stress becomes horizontal close to the ground surface, while the minor principal stress is vertical at depth.

5.3 Rock mass deformation

The thermal expansion of the rock mass surrounding the repository gives rise to a corresponding rock mass displacement in the outward direction (see Figure 5-7). In the model, and in reality, all surrounding boundaries are restrained except for the top surface (the ground surface); therefore, the displacements are largest upward.

This heave of the ground surface increases with time as a larger volume of rock mass expands. The magnitude of the heave also depends on the geometry of the repository. Figure 5-8 compares the maximum heave for different repository layouts. The two cases giving the highest values (2_50 and 3_150) have their repository levels closest to the ground surface, as compared to the other layouts. (The upper level of 3_150 lies at 400 meters depth; see Table 2-1). The smallest heave (16.5 cm) was obtained for the single-level repository.

As already mentioned, the thermal expansion and the corresponding rock displacements cause a destressing of the rock mass at shallow depth. In the main model, where the rock mass is assumed to have no tensile strength, the stress decrease leads to tensile yield in this area. In *3DEC*, the location of zones yielded during the calculations may be plotted; one example is shown in Figure 5-9. This figure shows the result for the main model and illustrates how a destressed area close to the ground surface develops above the repository. Other models show a similar pattern, but with tensile yield down to different depths (see Section 6).

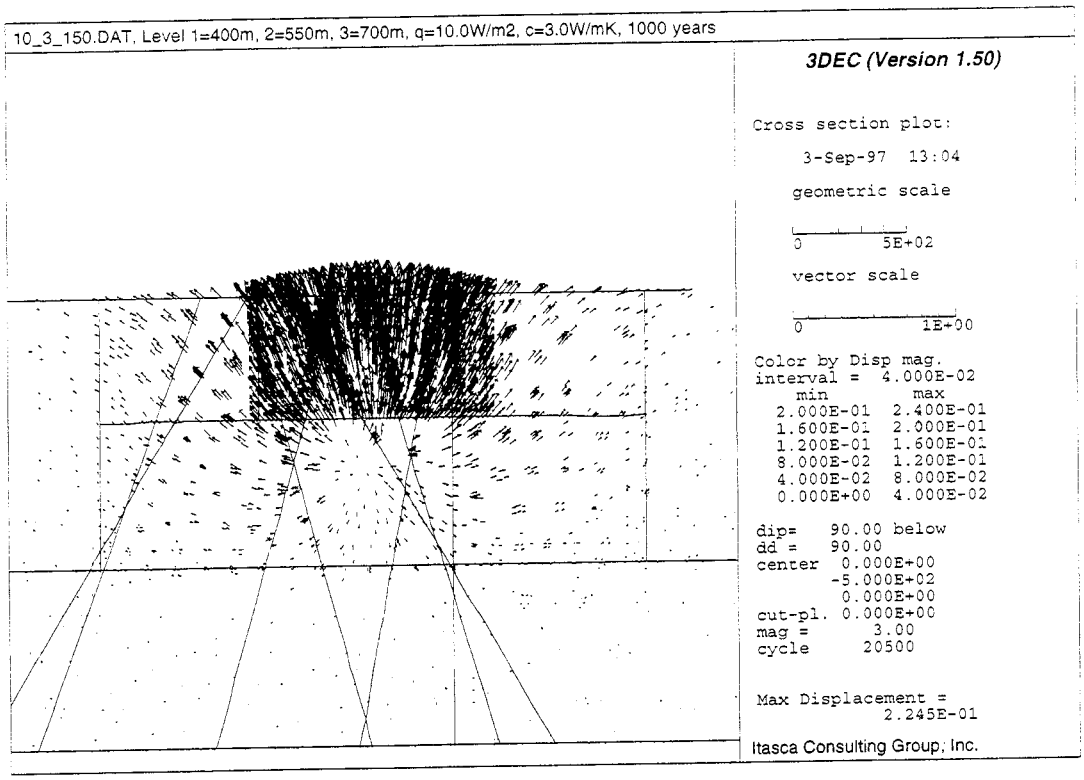

Figure 5-7. *Displacement plot on vertical section through the model for the case 3_150 at 1000 years.*

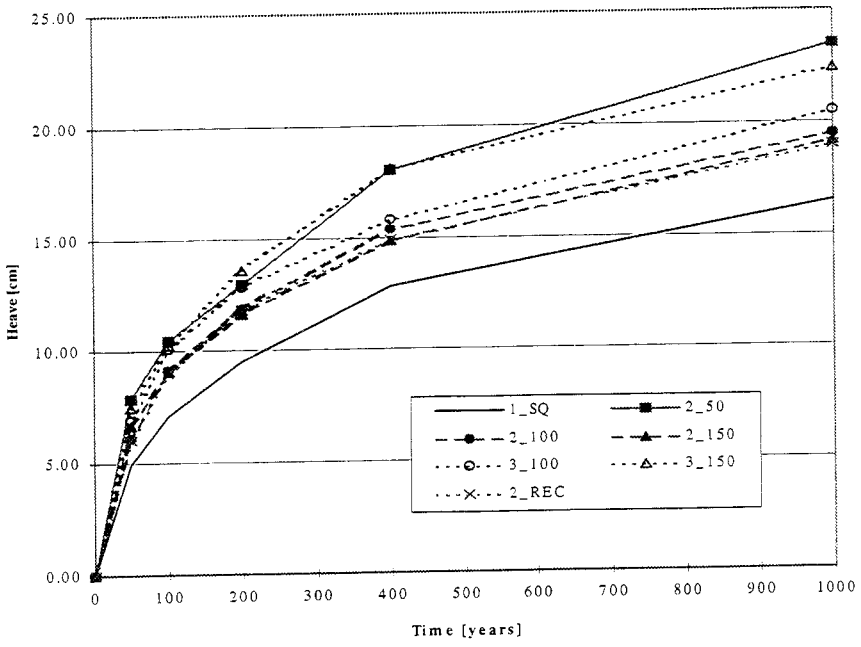

Figure 5-8. *Heave of ground surface at a point above the repository center versus time after deposition for different repository layouts (see Table 2.1). (The heat intensity assumed is 10 W/m² on each level.)*

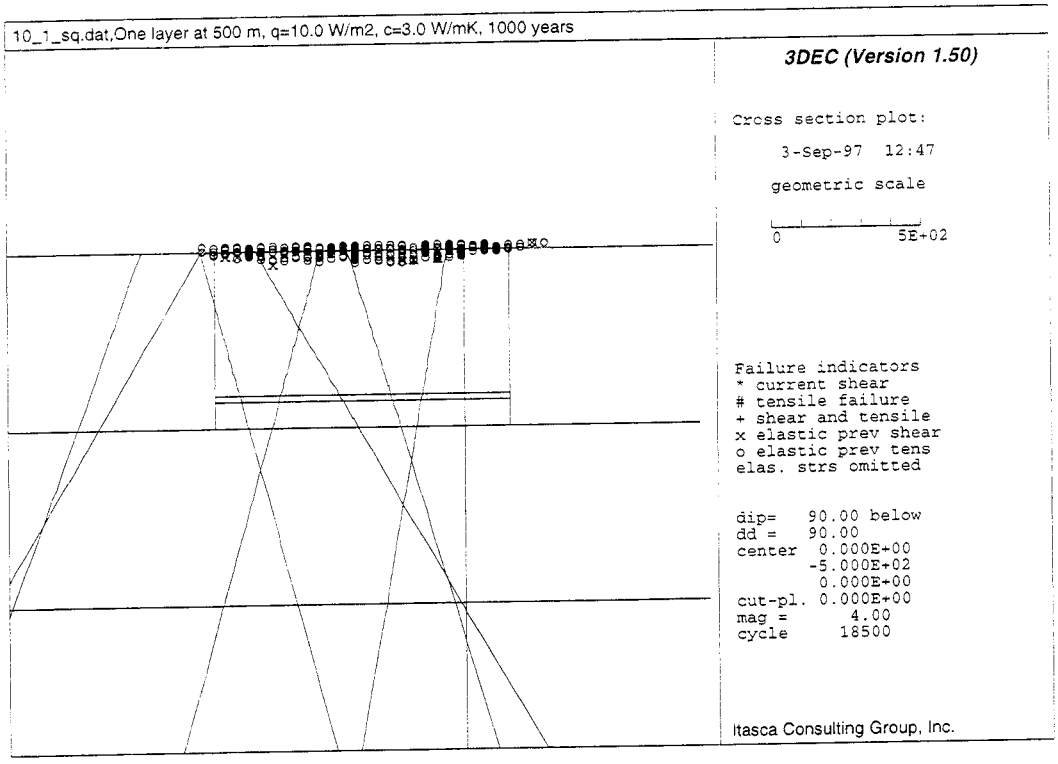

Figure 5-9. *The location of zones that have yielded during the calculation (after 1000 years of deposition), illustrating the destressed area that develops close to the ground surface for a single-level repository at 500-m depth (1_SQ). (The horizontal and vertical solid lines in the model are region boundaries, and the inclined lines are the fracture zone intersections with the vertical section.)*

5.4 Fracture zone deformation

The fracture zone displacement varies both spatially, over the fracture zone area, and with time. Figures 5-11a and 5-11b show examples of calculated fracture zone displacements plotted in a vertical section of the model. The largest closing displacements can be seen at the repository level; displacements in the opening direction occur at shallower depth, in correspondence with the changes in stress distribution as presented above.

Differences in location, orientation and stiffness explain the differences in displacement magnitudes between fracture zones. Fracture zones not intersecting the repository, for example, will experience smaller displacements at a later stage. The largest displacements calculated on each fracture zone are compiled in Table 5-1. These maximum values may refer to different times analyzed. They may also refer to different repository layouts, but are all from models with an initial thermal load of 10 W/m^2 and E = 30 GPa. (For a detailed description of fracture zone displacements, see *[Israelsson. 1996a]* and *[Israelsson et al.,1997a]*).

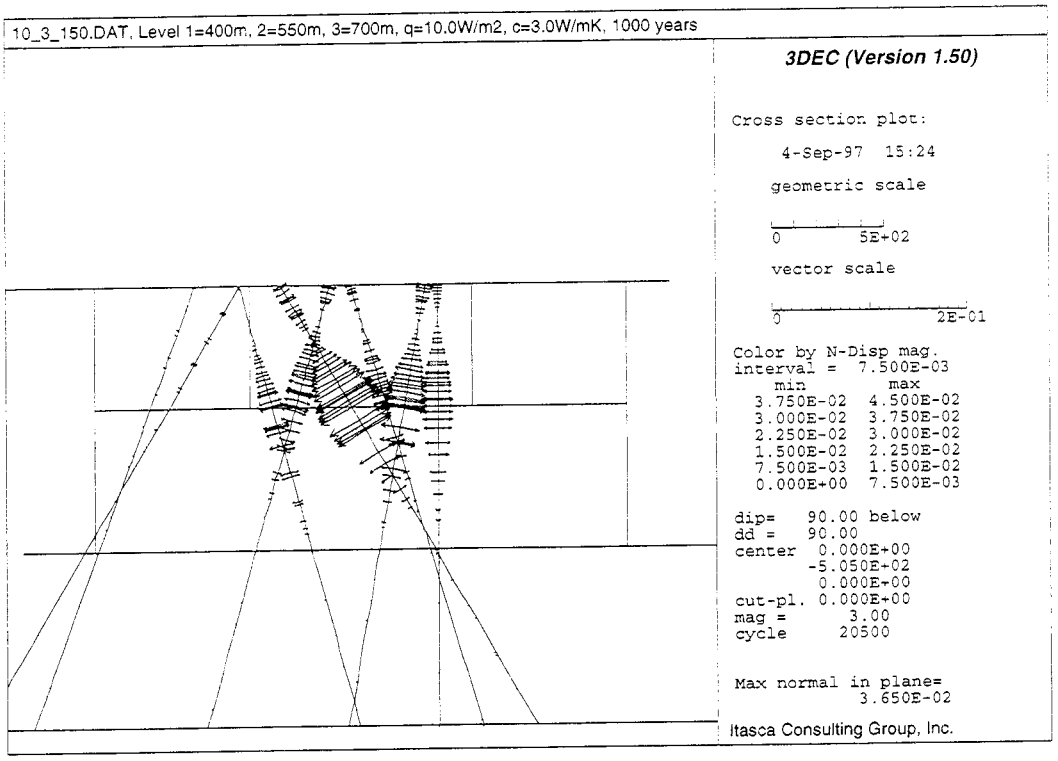

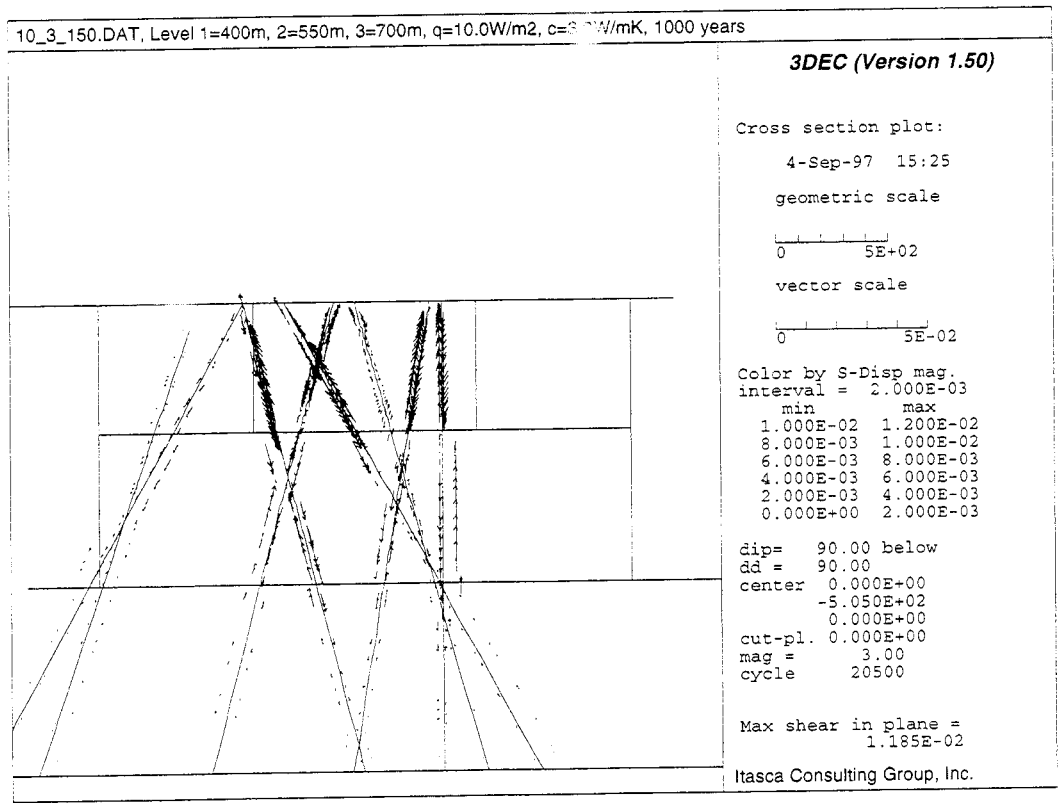

Figure 5-11. *a) Normal and b) shear displacements along fracture zones on a North-South-orientated vertical section. (Note that the vector lengths correspond to the absolute values of the displacement magnitudes (closing at depth and opening near the ground surface). Layout is 3_150. 1000 years after deposition.)*

It can be noted from Table 5-1 that all maximum displacements are in the range from zero to five centimeters, where the closing displacements are the largest and the opening displacements smaller. These displacement magnitudes should be related to the width of the deforming fracture zones, which are up to 30 meters. The pattern of fracture zone displacement is fairly consistent between different models analyzed, which should be expected since the stiffness of the fracture zones was not changed.

Table 5-1. Maximum observed displacements of the fracture zones.

Fracture Zone	Maximum Closure [cm]	Maximum Opening [cm]	Maximum Shearing [cm]
EW-1n	2.7	0.8	1.4
EW-1s	3.2	1.0	1.4
EW-3	2.2	0.8	1.1
EW-7	0.2	0.0	0.2
NE-1	4.5	0.9	2.7
NE-2	1.8	0.5	1.0
NE-3	2.2	0.3	1.4
NE-4	0.4	0.2	0.5
NNW-4w	2.5	0.5	1.0

6 SENSITIVITY ANALYSIS

6.1 Geological model set-up

Three different fracture zone geometries were used for the initial *3DEC* modeling. The models were named A, B and C and included 2, 4 and 9 fracture zones respectively (see Figure 6-1). These analyses were performed to investigate the influence of the fracture zones.

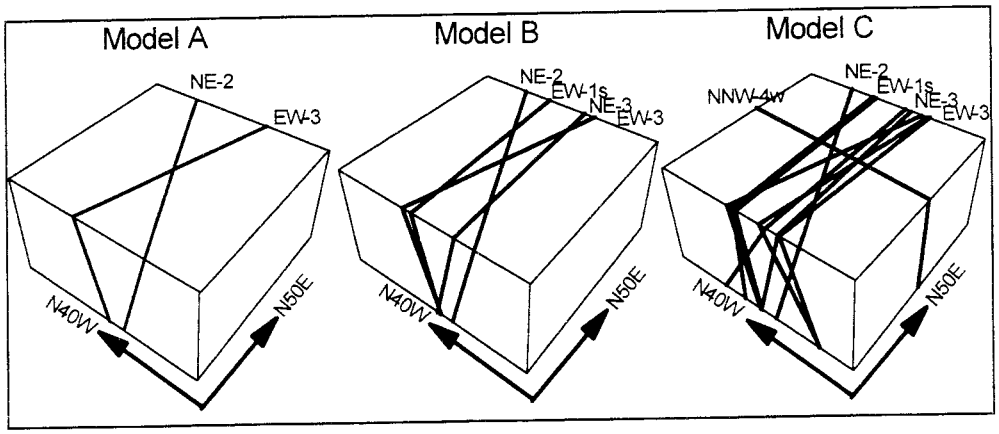

Figure 6-1 *Fracture zone geometry in Models A, B and C.*

The results of this comparison are presented in Table 6-1 and Table 6-2, which show the change in major principal stress at the repository level and the change in minor principal stress at the ground surface, respectively. A continuum model produces the largest stress increase at the repository level. In the *3DEC* models, the stress increase gradually becomes smaller with more fracture zones included. The increase of σ_1 for the Model C is approximately 30% smaller than that obtained in the Model-A analyses. It should be noted that these results are from models with high Young's modulus, E = 60 GPa.

Table 6-1. Maximum change in major principal stresses at the repository level, between deposition tunnels (500-m depth).

Time, t, after deposition [years]	σ_1 (t) - σ_1 (t=0) [MPa]			
	Heat intensity 6.0 W/m^2			Heat intensity 10.0 W/m^2
	Model A	Model B	Model C	Model C
100	15.8	14.7	10.9	18.0
400	15.6	14.2	10.8	18.0
1000	12.9	11.6	9.1	15.1

Table 6-2. Maximum change in minor principal stresses 5 m below ground surface.

Time, t, after deposition, [years]	σ_3 (t) - σ_3 (t=0) [MPa]			
	Heat intensity 6.0 W/m^2			Heat intensity 10.0 W/m^2
	Model A	Model B	Model C	Model C
100	-0.4	-0.3	-0.2	-1.6
400	-2.7	-3.0	-2.1	-2.9
1000	-3.9	-4.3	-3.0	-4.1

The major principal stress is always oriented horizontally; the minor stress is vertical at depth and horizontal at shallow depths. At the ground surface, the principal stresses decrease, and the minor stress becomes tensile. It should be noted that, in these models, the rock was assumed to have a tensile strength of 8.7 MPa. The horizontal stress decreases by about 5 MPa at the ground surface 1000 years after deposition. The major principal stresses also decrease to approximately zero close to the ground surface after 1000 years of deposition

Even though the number of fracture zones in the model influences the stress magnitudes, no major stress rotations or redistributions can be seen as a result of fracture zones cutting through the rock mass. The explanation to this is that most fracture zones behave elastically within the time span studied and that all boundary surfaces, except the top surface, are fixed in their normal directions. Another reason is that the orientation of the fracture zones are subparallel to the principal stress directions.

6.2 Boundary conditions

Ideally, the size of a numerical model is large enough so that the boundary conditions will not affect the area of interest. However, in this study, the global effects have been studied, and it was expected that a change in boundary condition from fixed normal displacement to fixed normal stress

conditions would give slightly different results. Therefore, these two different boundary conditions for the vertical boundaries of the *3DEC* model were compared.

The results show that stress levels change slightly with changed boundary condition. In general, the fixed displacement condition gives higher stress levels. The two curves in Figure 6-2, for example, present the calculated minor principal stress along the vertical scanline. The stress boundary gives a slightly deeper area of tensile stresses (~100 m compared to ~90 m). The stress-boundary case also results in 20-40 % larger opening and shear displacements at the ground surface for some of the fracture zones (NNW-4w, EW-3, NE-1 and NE-2). At the repository horizon, there is a slight decrease in displacements for some of the fracture zones.

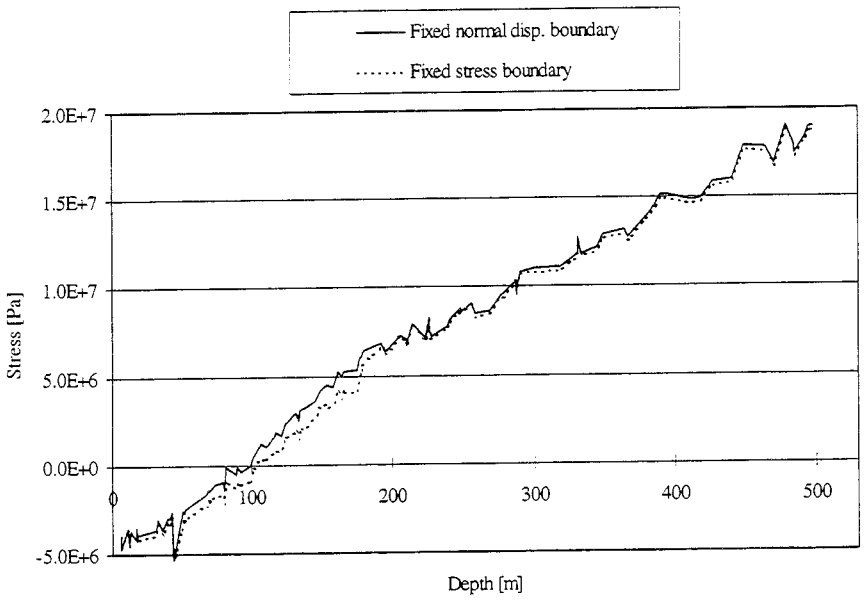

Figure 6-2. *Minor principal stress versus depth at the center of the repository for a 3DEC model with different boundary conditions on the outer vertical boundaries. (The solid line is the result with zero normal displacement; the dashed line is the results with constant stress boundaries. The two models are otherwise identical.)*

6.3 Material properties

In addition to the model geometry and the boundary conditions, the material properties are important factors influencing results. In the initial *3DEC* model, the rock mass was assumed to have a tensile strength of 8.7 MPa (to facilitate comparison with *STRES3D* models). It was judged, therefore, that a material without tensile strength would better represent the actual rock mass material, since the blocks in the *3DEC* models are not simulating intact rock blocks but, rather, rock mass volumes between fracture zones.

Analyses performed with and without tensile strength were compared; the main difference was, as expected, seen in the stresses in the rock mass close to the ground surface. In this shallow region, tensile yield develops and the minor stress is correspondingly kept at zero (see Figure 6-3).

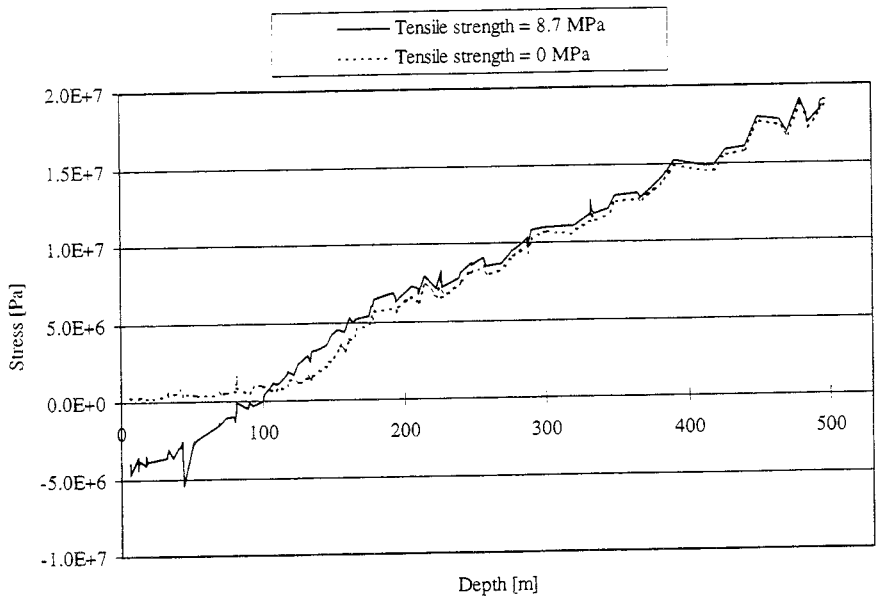

Figure 6-3. *Minor principal stress versus depth at the center of the repository for a 3DEC model with rock blocks with and without tensile strength, respectively. (Negative values of minor stress indicates tensile stress.)*

A similar comparison was also carried out for a change in the Young's modulus of the rock mass blocks. One of the two values used was 60 GPa, which is regarded as a high value; the other value chosen was 30 GPa. The differences in results between these two cases are quite large, as can be seen from the stress versus depth curves in Figure 6-4 and Figure 6-5.

The maximum major principal stress at the repository level is, for example, about 44 MPa using the lower Young's modulus and about 52 MPa with the high modulus. The initial major principal stress is about 32 MPa.

With a lower value of Young's modulus, all mechanical effects will be less in areas far from the repository, and the extent of destressed rock at the ground surface will also be correspondingly decreased. The depth to which tensile stresses occur, for the case with E = 30 GPa, is reduced by about 50% compared to the case with E = 60 GPa (see Figure 6-5). (In both these models, a tensile strength of 8.7 MPa is assumed for the rock blocks.)

Accordingly, a major reduction of both normal and shear displacements of the fracture zones are obtained with E=30 GPa. At the repository level, closure of the zones is reduced by 30-40%, compared to the case with

E = 60 GPa. At the ground surface, the opening normal displacements are also reduced around 50%.

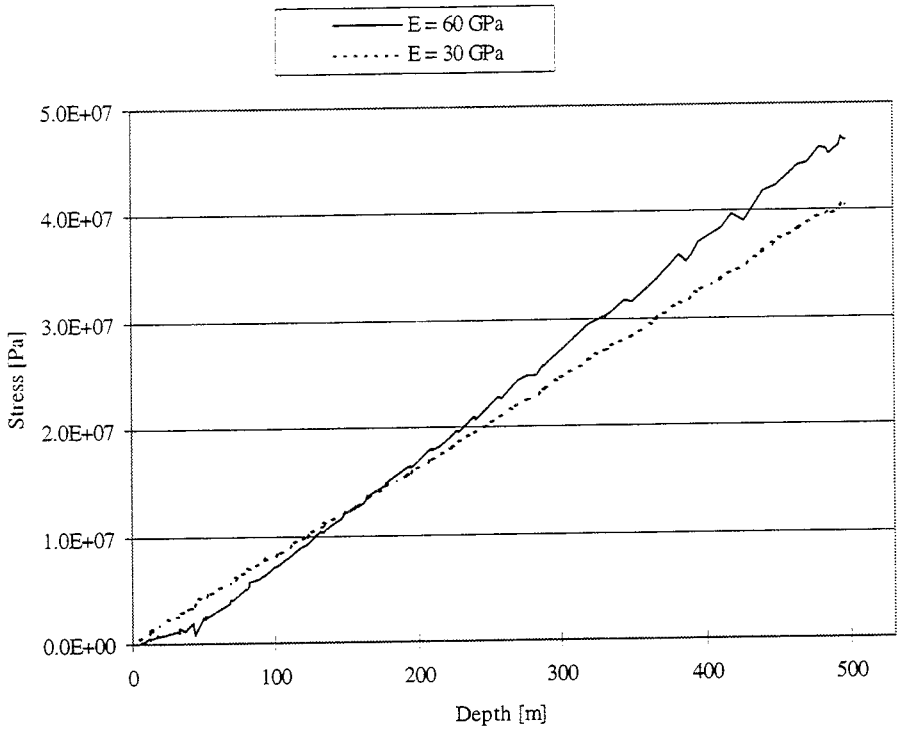

Figure 6-4 *Major principal stress versus depth at the center of the repository for a 3DEC model with different Young's modulus in the rock blocks (see legend). (The two models are otherwise identical.) (1000 years of deposition).*

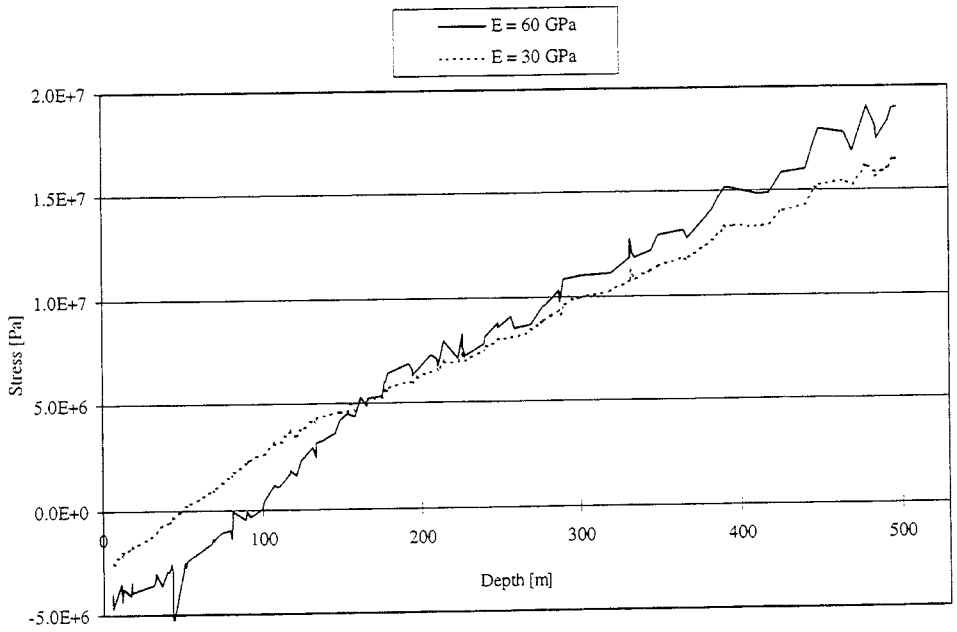

Figure 6-5 *Minor principal stress versus depth at the center of the repository for a 3DEC model with different Young's modulus in the rock blocks (see legend). (The two models are otherwise identical.)*

6.4 Effects of excavation openings

In the main modeling work for this study, the repository was only simulated in terms of the thermal load from the heat generating canisters. The repository will further influence the surrounding rock with the excavation of tunnels and deposition-hole openings. The tunnels and deposition holes will cause stress reorientation and local deformation towards the openings.

To investigate how much the excavations could influence the thermo-mechanical effects on the rock on a global scale, an additional *3DEC* analysis was performed *[Israelsson et al., 1997b]*. In this *3DEC* model, a tabular region of 24-m height, corresponding to the repository effective height, was given lower material properties to simulate the more compliant behavior of this horizon due to the excavations. The material model was still kept as an isotropic Mohr-Coulomb material.

A *UDEC* (two-dimensional distinct element code) *[Itasca, 1996]* model was used to calculate the most appropriate "equivalent" material properties to be used for the repository region. The model consisted of a rectangular "unit" volume of rock (24 x 20 m) with one tunnel opening (4 x 4 m) in the center. This rock "sample" was loaded numerically in horizontal and vertical directions, and the stresses and strains were monitored (see Figure 6-6 and Figure 6-7). The rock was modeled as an isotropic continuum. Several models with different confining stress were analyzed.

In this way, the yield curve for the "composite material" (rock + tunnel) could be constructed, and the values selected for the repository region in the *3DEC* model are listed in Table 6-3.

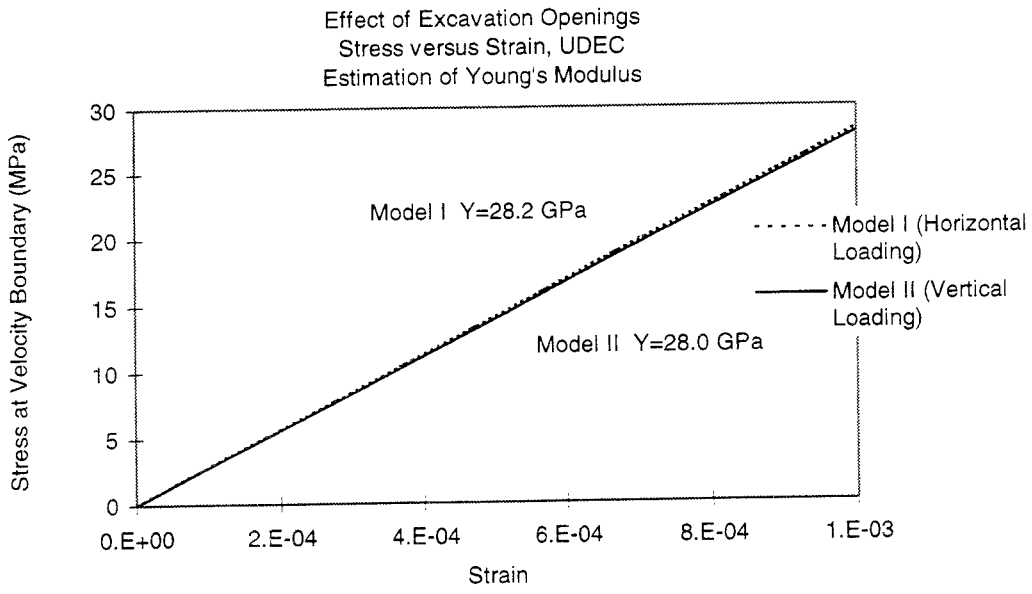

Figure 6-6. *Stress versus strain curves for Model I and II. (Estimated values of Young's modulus for the two models are given in the graph.)*

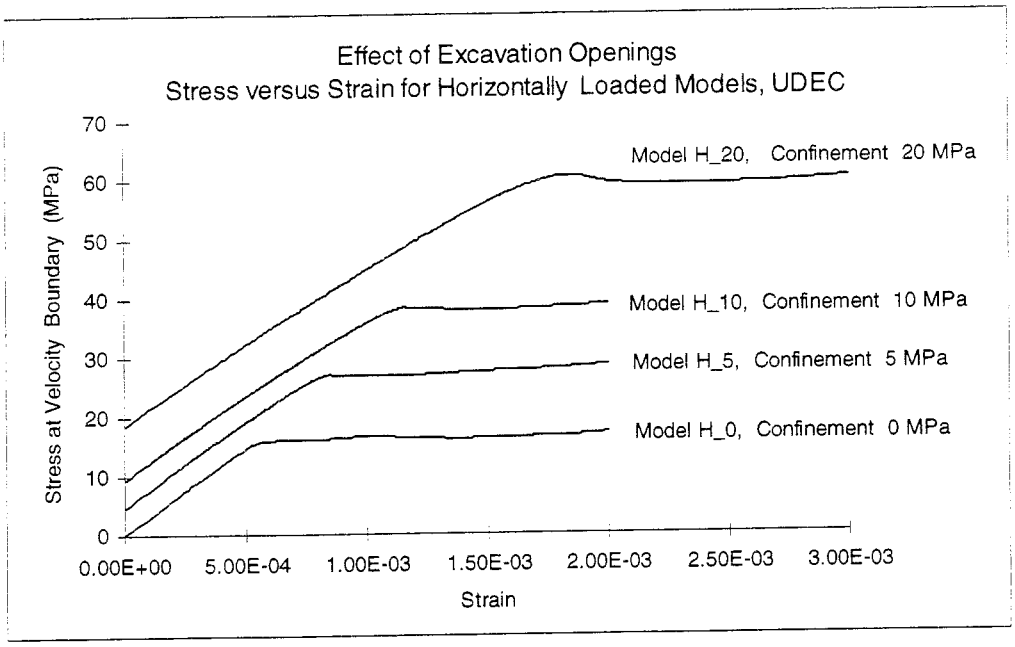

Figure 6-7. *Stress versus strain curves for models loaded horizontally.*

The Young's modulus of the rock mass in the repository region is lowered only slightly, from 30 to 28 GPa. The friction angle is reduced clearly from 30 to 19 degrees.

The stress distribution and displacements calculated are almost identical in areas outside the repository region. In the elements of the repository region itself, the effects of lower strength can be observed. In a plot of yielded volumes, it can be noted that, apart from the shallow near surface area, yield also occur in the repository area (Figure 6-8).

The very small influence on the global behavior may be illustrated by the curves for ground surface heave as it develops with time (Figure 6-9). After 1000 years, the case that considers excavation openings has an insignificantly higher value than the main model.

Table 6-3. Rock mass properties used in the *3DEC* model.

Rock Mass Properties	Surrounding Rock Mass	Rock Mass in the Repository Region
Young's modulus [GPa]	30	28
Poisson's ratio	0.22	0.22
Cohesion [MPa]	5	5.3
Friction angle [°]	30	19
Tensile strength [Pa]	0	0

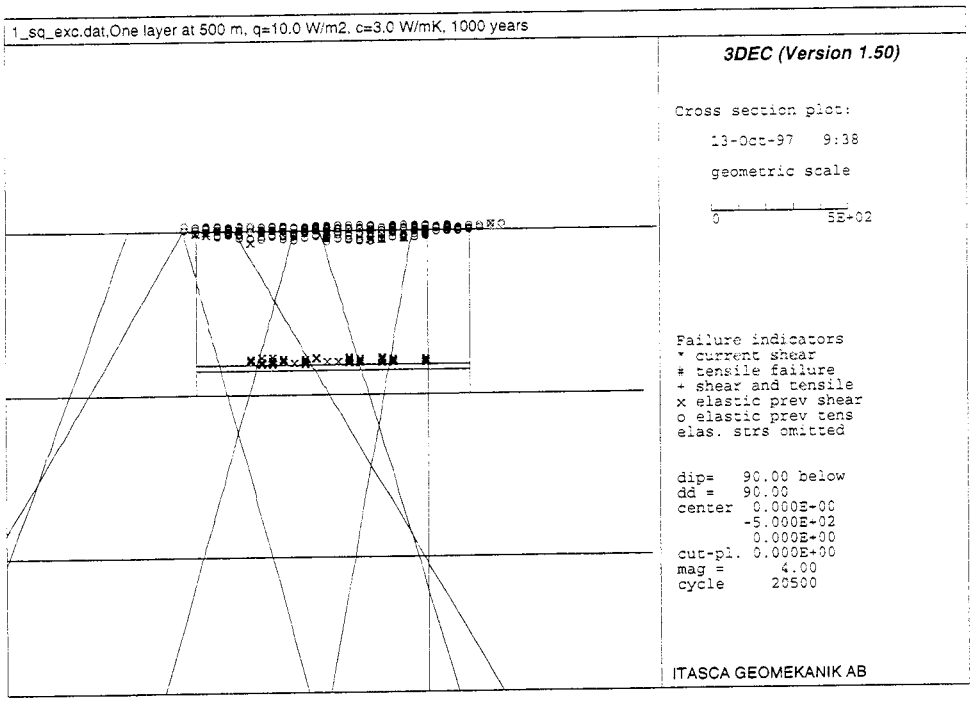

Figure 6-8. *Zones yielded in tension and shear at the vertical cross-section 1000 years after deposition for the model with equivalent properties in the repository region (1_EXC).*

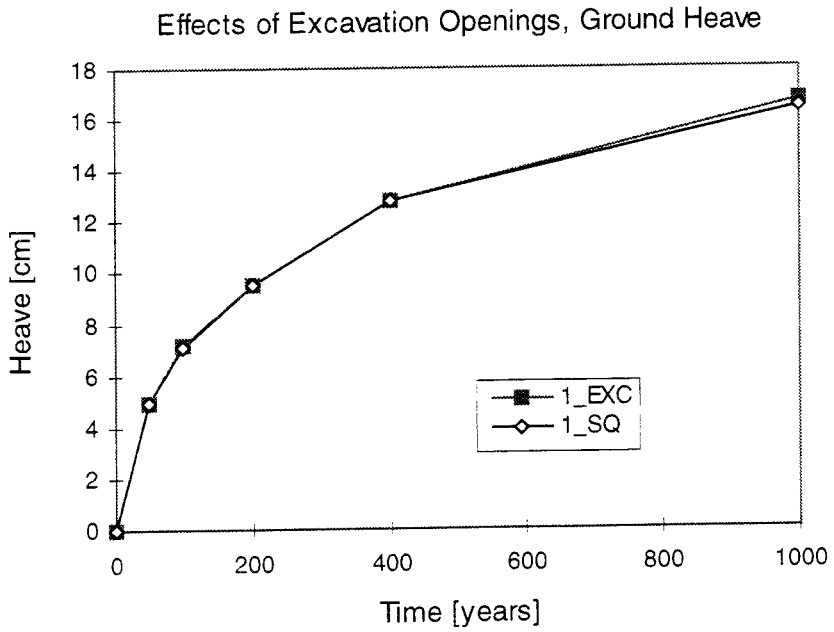

Figure 6-9. *Ground heave above center of repository versus time after deposition for a model with a repository region with reduced strength (1_EXC) and a model with uniform properties (1_SQ).*

7 DISCUSSION

7.1 Temperature distribution

The thermal conductivity of the rock mass restrains the heat front from moving quickly. The shallow rock horizons and the rock deep below the repository thus experience maximum temperatures long after the maximum temperature is reached at the repository horizon. Therefore, the different thermo-mechanical effects that result from the temperature increase continue to grow slightly even after 1000 years in areas far from the repository.

It has been shown that the heat-intensity decay function (eqn. 3-1) is accurate up to about a 1000 years, but it loses its accuracy in predicting heat intensity degradation afterward *[Thunvik and Braester, 1991]*. Therefore, calculations in this study have not been extended beyond 1000 years. To fully monitor stresses and displacements covering the peak response and the cooling phase, a somewhat longer time period should be studied.

The values of maximum temperature reported here refer to the maximum value along the vertical scanline, which passes through the center of the repository in between two tunnels. This means that the calculated temperatures correspond to a point in the rock mass about 20 meters away from the canisters. The maximum temperatures close to the canister are higher. The detailed distribution of temperatures near the repository should be discussed based on modeling on a smaller scale (e.g., *[Vallander, 1995]*, *[Pusch and Hökmark, 1991]*).

7.2 Stress distribution

The calculations were made without considering pore pressures, which would produce effective stresses that are less than the total stresses by the magnitude of the pore pressures and thus move the state of stress toward the yield envelope. If pore pressures were included, the displacements of rock and fracture zones might still show the same pattern at the repository level, since the response there is in the elastic regime. Closer to the ground surface, where tensile yield occurs, including pore pressure in the simulation might expand the area of tensile yield.

The assumptions about the constitutive model and the input parameters influence the modeled rock mass behavior, particularly at the ground surface. At the repository horizon, the conditions are less sensitive to the different variations made in this study. The most important parameter in this respect is the Young's modulus. By halving the Young's modulus, peak

stresses developing from the thermal expansion of the rock are reduced; this also results in reduced yielding of the shallow rock.

In the primary analysis, a very high value of Young's modulus was used (60 GPa), which is of the order of the intact rock modulus. In the scale of the modeled volume, rock mass blocks with sizes of hundreds of meters would have lower stiffness than intact rock due to the fractures. It is therefore likely that the lower value for the Young's modulus (30 GPa) used in much of this study is more appropriate for prediction, although this is not the most conservative choice.

A heave of the rock mass is one of the observed effects of thermal load. The heave, as such, is not expected to be critical for the safety assessment of a KBS-3 repository, but the corresponding re-orientation of stresses and deformations may alter the transport properties of the area and should therefore be factors included in the assessment. At the ground surface, above the repository center, the monitored displacements are the accumulated displacements from the entire heated rock mass below and thus represents the maximum vertical displacement. The displacements in other directions are less because of the confining tectonic stresses. Because the large distance of 500 metrs, it takes more than a thousand years for the thermal effect to fully develop close to the ground surface .

Based on the observations of the Äspö geology, it may also be noted that the "geological models" considered in this study all have fracture zones with subvertical dip. In a more general study, one could consider also having horizontal or gently dipping structures located between the repository and the ground surface and/or having a rock mass with depth-dependent Young's modulus. Such changes in the geological model might result in changes in the predictions of the global thermo-mechanical effects.

7.3 Fracture zone displacements

During the long-term thermo-mechanical loading of the rock mass in its global scale, the fracture zones undergo closure, opening and shearing displacements. From the perspective of the mechanical stability of a repository, these movements are advantageous, since some of the stresses are relieved. Closure of the fracture zones in the neighborhood of a repository is also advantageous with respect to hydraulic properties. On the other hand, the opening of fracture zones at shallow depth may enhance the groundwater movement in this area. Shear displacements of the fracture zones may or may not play a significant role on the groundwater movement depending on the dilatational characteristics of those zones. These aspects may be better understood when future studies in the context of coupled hydro-mechanical processes are carried out.

As a part of the safety assessment, criteria concerning acceptable levels of displacement must be determined for the fracture zones. Because the actual

effects on the transport properties from fracture displacement are difficult to determine, one possible criterion could be that limited fracture zone displacements in the opening direction are accepted if they occur in areas where the properties of the rock mass are not critical for the assessment. The calculations performed in this study, using a conservative value on heat intensity, indicate that the main area of possible increase in hydraulic conductivity of fracture zones (compared to initial conditions) lies from the ground surface down to a maximum depth of about 200 meters, 300 meters above the repository level.

7.4 Effect of excavation openings

In the *UDEC* modeling that was performed to estimate suitable equivalent material properties at the repository level, simulating the effects of excavation openings, the distance between the tunnels was 20 meters. In the original layout for a KBS-3 type repository, the distance between deposition tunnels is 40 meters. Thus, the use of 20 m is conservative, giving a larger difference between the rock in the repository horizon and the surrounding rock mass than would be expected with 40 m distance between tunnels. Still, this modeling resulted in a fairly small reduction of the strength parameters estimated for the repository region.

Because there is great general uncertainty in selecting input parameters for a large rock area (e.g., E-modulus and fracture zone stiffness), the span of potential thermo-mechanical effects becomes large. The selection of properties of the repository region should also be viewed in this context. The reductions estimated, due to excavation openings, may well be of the same order as the natural variation of strength parameters in the rock mass.

In the present "global scale" study, the approach was that the effect of excavation openings could be simulated in the model with a tabular region having homogenous, isotropic material properties (without excavations). In reality, the stresses and strains in the rock mass closely surrounding the tunnels and deposition holes will vary strongly depending on the location with respect to the openings. Therefore, the stresses and strains calculated in this study cannot be used for discussions of any "near-field" conditions.

Also, the heat flux in this global study was simplified geometrically. The heat-generating canisters were simulated as point heat sources, and the thermal properties of bentonite and other filling material were neglected. This study does thus not allow for discussions concerning the detailed temperature distribution within the repository horizon. It is suggested that further studies be carried out to investigate the thermo-mechanical effects on a smaller scale with excavations modeled explicitly.

8 CONCLUSIONS

8.1 Predicted temperatures, stresses and displacements

For a single-level repository, the temperature reaches a maximum of 70 °C (from an initial 15 °C) during 100–400 years after deposition, considering a vertical scanline about 20 meters from the deposition holes between the tunnels. (Note that an initial thermal load of 10 W/m^2 is assumed for this model). Far from the repository, the temperature still increases slightly after 1000 years of deposition. The maximum temperature thus occurs at different times depending on the location considered.

As a result of the thermal loading at the repository, the state of stress is progressively changed. In general, the principal stresses increase near the repository, closing the fracture zones at that vicinity. The volume around the repository within which fracture zones close increases with time. The maximum principal stress obtained for the main model is 44 MPa and occurs at the repository level after about 100 years. The main model is the model with 9 fracture zones and a Young's' modulus of 30 GPa (cf. section 8.2). After 1000 years of deposition, the stresses have decreased just slightly.

At the ground surface, a stress reduction of approximately 5 MPa can be found 1000 years after deposition (for areal heat intensity 10.0 W/m^2). The reduction of the minor principal stress at the ground surface causes the rock to yield in tension down to a depth of 80 meters (Tensile strength is assumed to be zero.), which may result in a change of the transport properties in this zone.

The fracture zones also exhibit opening displacements at shallow depths due to the normal stress decrease. Closer to the repository, the fracture-zone displacements are closing and shearing. The magnitudes of maximum displacements for the different fracture zones, are 0.3-2.5 cm for closing, 0.0-0.8 cm for opening and 0.2-2.2 cm for shearing, respectively.

8.2 Influence from model assumptions and parameters

The magnitudes of the stress changes and displacements calculated depend on the assumptions made concerning heat intensity and heat intensity function. The 10 W/m^2 loading does result in clearly larger thermo-mechanical effects than the thermal load of 6 W/m^2 does (e.g., the major stress encountered along the scanline increases up to 50 MPa and up to 42

MPa, respectively; Initially σ_1 = 32 MPa. Note that this comparison was made with models having Young's Modulus E= 60 GPa).

Another important input parameter for the resulting thermo-mechanical effects is the Young's modulus for the rock blocks. For example, the closure of fracture zones around the repository decreases by 40% when the Young's modulus is lowered to 30 GPa from 60 GPa. Also, the stress release at the ground surface is less with the lower Young's modulus. Other changes of material properties considered give minor changes of the behavior.

8.3 Influence of fracture zones

The predicted stress at the repository level becomes highest for a continuum, elastic assumption and gradually decreases as more fracture zones are included in the analysis. The increase of σ_1 due to heating at the repository center is, for the main model (*3DEC*), about half that obtained with the corresponding purely elastic analyses (50 MPa compared to 66 MPa for a heat intensity of 10.0 W/m^2 and E = 60 GPa).

The presence of major fracture zones in the rock mass could thus be important for the stress level reached at the repository, since peak stresses are reduced. The reason for this is the relatively low shear and normal stiffness of the fracture zones, which absorb deformations (and, thereby, stresses) that develop from heat-induced expansion. The inclusion of fracture zones does not cause any major changes in the orientation of stresses.

Because it is difficult to determine the stiffness of a fracture zone, the magnitudes of predicted displacements are uncertain. The stiffness assumed for each fracture zone in this study was maintained in all *3DEC* models.

8.4 Multi-level repository

All multi-level repository layouts analyzed give rise to higher temperatures in the surrounding rock mass than does the single-level layout (e.g., layout 2_50 gives a maximum of 115 °C at 400 years compared to 70 °C for 1-SQ). This also causes the compressive stresses to increase more at the repository level as compared to the single-level case. (Note that this applies when the areal heat intensity on each separate level is the same, 10 W/m^2).

The *3DEC* analyses further indicate that all of the multi-level layouts considered cause destressed zones extending in depth well beyond that induced by a single-level layout. Layouts 2_50 and 3_150 create similarly deep destressed zones (160 m and 150 m, respectively) that are deeper than those caused by other layouts (80 m for the single layout).

Shear displacement and opening or closing displacements normal to the fracture zones, caused by the different layouts, are so similar that no firm conclusions can be drawn that may favor any of the layouts based on those factors. The normal displacements of the fracture zones are in the opening direction down to depths of 135-325 meters below the ground surface, depending on the layout and the properties of the fracture zone in question. (Note that this does not mean that the normal stress over the fracture zone is zero but, simply, that it has decreased).

8.5 Effects of excavation openings

A *3DEC* model with altered properties at the repository region was analyzed to evaluate the influence from the excavation openings in the repository. The results show that extent and depth of the tensile yield near the ground surface and fracture zone displacements are very similar for the model with equivalent properties for the repository region and the model with uniform properties. It seems, therefore, that the thermo-mechanical effects of excavation openings on a global scale are not significant.

The *3DEC* model indicates that overstressed rock mass may be encountered locally in the repository region. However, the level of detail in the models in this study does not allow for any discussion in details on stresses and strains close to the repository excavations. Further studies on a smaller scale, with excavation of tunnels and canister holes modeled explicitly, are needed to study the presence and extent of overstressed rock mass in the repository region.

9 ACKNOWLEDGMENTS

The participation in the project reference group, by Prof. Ove Stephansson and Dr. Jing Lanru (Royal Institute of Technology, Stockholm), and the contributions they made throughout this project are acknowledged.

The acknowledgment is also extended to Dr. Loren Lorig (Itasca Consulting Group, Inc.) for his advice and comments and Ms. Kathy Sikora (Itasca Consulting Group, Inc.) for her editorial review.

10 REFERENCES

Almén, K-E., R. Stanfors and C. Svemar. (1996) "Nomenklatur och Klassificering av Geologiska Strukturer vid Platsundersökningar för SKB:s Djupförvar," SKB, PR D-96-029, Stockholm.

Gustafson, G., M. Liedholm, I. Rhén, R. Stanfors, and P. Wikberg. (1991) "Äspö Hard Rock Laboratory. Predictions Prior to Excavation and the Process of Their Validation," SKB, Technical Report 91-23, Stockholm.

Hansson, H., O. Stephansson, B. Shen and A. Lundin. (1995a) "Far-Field Rock Mechanical Modeling For Nuclear Waste Disposal," SKI, TR 95:40, Stockholm.

Hansson, H., L. Jing and O. Stephansson. (1995b) "3-D DEM Modelling of Coupled Thermo-Mechanical Response For a Hypothetical Nuclear Waste Repository," in ***Proceedings of the Fifth International Symposium on Numerical Models in Geomechanics (Davos, 1995)***, pp. 257-262.

Israelsson, J. (1995a) "Global Thermo-Mechanical Effects From a KBS-3 Type Repository — Phase 1: Elastic Analyses," SKB, PR D-95-008, Stockholm.

Israelsson, J. (1995b) "Global Thermo-Mechanical Effects From a KBS-3 Type Repository — Phase 1: Elastic Analyses, Full Set of Plots," SKB, AR D-95-004, Stockholm.

Israelsson, J. (1996a) "Global Thermo-Mechanical Effects From a KBS-3 Type Repository — Phase 2: Three-Dimensional Distinct-Element Modeling With Major Fracture Zones — Base Case," SKB, PR D-96-006, Stockholm.

Israelsson, J. (1996b) "Global Thermo-Mechanical Effects From a KBS-3 Type Repository — Phase 2: Three-Dimensional Distinct-Element Modeling With Major Fracture Zones — Base Case, Full Set of Plots," SKB, AR D-96-008, Stockholm.

Israelsson , J. (1997a) "Global Thermo-Mechanical Effects From a KBS-3 Type Repository — Phase 2a: Three-Dimensional Distinct-Element Modeling With Major Fracture Zones — Sensitivity Analyses," SKB, PR D-97-001, Stockholm.

Israelsson, J., H. Hakami and E. Hakami. (1997a) "Global Thermo-Mechanical Effects From a KBS-3 Type Repository — Phase 3a: Multilevel Repository," SKB, Progress Report PR D-97-10, Stockholm.

Israelsson, J., H. Hakami and E. Hakami. (1997b) "Global Thermo-Mechanical Effects From a KBS-3 Type Repository _ Effect of Excavation Openings," SKB, Project Report, PR D-97-11, Stockholm. (Note: The first names of the authors printed on this report are erroneously given; the correct names should have been S.-O. Olofsson and E. Hakami.)

Itasca Consulting Group, Inc. (1994) ***3DEC Version 1.50.*** Minneapolis, Minnesota: ICG.

Itasca Consulting Group, Inc. (1996) ***UDEC Version 3.0.*** Minneapolis, Minnesota: ICG.

Larsson, H. (1995) Personal Communication, SKB, Stockholm.

Munier, R. and H. Sandstedt. (1994) "SR-95: Hypothetical Layout Using Site Data From Äspö," SKB, Working Report 94-53, Stockholm.

Pusch, R., and O. Touret. (1988) "Heat effects on Soft Na Bentonite Gels," *Geologiska Föreningens i Stockholm Förhandlingar,* ***110*** (2) 183-190.

Pusch, R., and L. Börgesson. (1992) "PASS — Project on Alternative Systems Study. Performance Assessment of Bentonite Clay Barrier in Three Repository Concepts: VDH, KBS-3 and VLH," SKB, Technical Report TR 92-40, Stockholm.

Pusch, R., and H. Hökmark. (1991) "Characterization of nearfield rock — A basis for comparison of repository concepts," SKB, Technical Report 92-06, Stockholm.

SKB. (1992) "Project on Alternative Systems Study (PASS), Final Report," Technical Report 93-04, Stockholm.

Stephansson, O. (1995) Personal Communication, Royal Institute of Technology, Stockholm.

St. John, C., and M. Christianson. (1980) "*STRES3D* — A Computer Program For Determining Temperatures, Stresses, and Displacements Around Single or Arrays of Constant or Decaying Heat Sources," University of Minnesota, Report to Rockwell International, RHO-BWI-C-78.

Thunvik, R., and C. Braester. (1991) "Heat Propagation From a Radioactive Waste Repository — Complementary Calculations for the SKB 91 Reference Canister," SKB, Working Report TR 91-17, Stockholm.

Vallander, P. (1995) "Avstånd mellan kapslar bestämt av tillåten temperatur i omgivande kompakterad bentonit," SKB, Arbetsrapport AR D-95-006, Stockholm.

Windelhed, K., M. Alestam and I. Markström. (1995) "Bygganalys för SR 95 (in Swedish)," SKB, Djupförvar Arbetsrapport AR D-95-009, Sydkraft Konsult AB, Malmö.

List of SKB reports

Annual Reports

1977-78
TR 121
KBS Technical Reports 1 – 120
Summaries
Stockholm, May 1979

1979
TR 79-28
The KBS Annual Report 1979
KBS Technical Reports 79-01 – 79-27
Summaries
Stockholm, March 1980

1980
TR 80-26
The KBS Annual Report 1980
KBS Technical Reports 80-01 – 80-25
Summaries
Stockholm, March 1981

1981
TR 81-17
The KBS Annual Report 1981
KBS Technical Reports 81-01 – 81-16
Summaries
Stockholm, April 1982

1982
TR 82-28
The KBS Annual Report 1982
KBS Technical Reports 82-01 – 82-27
Summaries
Stockholm, July 1983

1983
TR 83-77
The KBS Annual Report 1983
KBS Technical Reports 83-01 – 83-76
Summaries
Stockholm, June 1984

1984
TR 85-01
Annual Research and Development Report 1984
Including Summaries of Technical Reports Issued during 1984. (Technical Reports 84-01 – 84-19)
Stockholm, June 1985

1985
TR 85-20
Annual Research and Development Report 1985
Including Summaries of Technical Reports Issued during 1985. (Technical Reports 85-01 – 85-19)
Stockholm, May 1986

1986
TR 86-31
SKB Annual Report 1986
Including Summaries of Technical Reports Issued during 1986
Stockholm, May 1987

1987
TR 87-33
SKB Annual Report 1987
Including Summaries of Technical Reports Issued during 1987
Stockholm, May 1988

1988
TR 88-32
SKB Annual Report 1988
Including Summaries of Technical Reports Issued during 1988
Stockholm, May 1989

1989
TR 89-40
SKB Annual Report 1989
Including Summaries of Technical Reports Issued during 1989
Stockholm, May 1990

1990
TR 90-46
SKB Annual Report 1990
Including Summaries of Technical Reports Issued during 1990
Stockholm, May 1991

1991
TR 91-64
SKB Annual Report 1991
Including Summaries of Technical Reports Issued during 1991
Stockholm, April 1992

1992
TR 92-46
SKB Annual Report 1992
Including Summaries of Technical Reports Issued during 1992
Stockholm, May 1993

1993
TR 93-34
SKB Annual Report 1993
Including Summaries of Technical Reports Issued during 1993
Stockholm, May 1994

1994
TR 94-33
SKB Annual Report 1994
Including Summaries of Technical Reports Issued during 1994
Stockholm, May 1995

1995
TR 95-37
SKB Annual Report 1995
Including Summaries of Technical Reports Issued during 1995
Stockholm, May 1996

1996
TR 96-25
SKB Annual Report 1996
Including Summaries of Technical Reports Issued during 1996
Stockholm, May 1997